Testicular biodistribution of 450 nm fluorescent latex particles after intramuscular injection in mice.

Jean-Philippe Klein, Delphine Boudard, Josette Cadusseau, Sabine Palle, Valérie Forest, Jérémie Pourchez, Michèle Cottier

Testicular biodistribution of 450 nm fluorescent latex particles after intramuscular injection in mice

J-P. Klein[1, 2, 3, 4, 5], D. Boudard[1, 2, 3, 4, 5], J. Cadusseau[6], S. Palle[4, 7], V. Forest[1, 3, 8], J. Pourchez[1, 3, 8], M. Cottier[1, 2, 3, 4, 5]

[1] LINA, EA 4624, F-42023, Saint-Etienne, France

[2] Université Jean Monnet, Faculté de Médecine, F-42023, Saint-Etienne, France

[3] SFR IFRESIS, F-42023, Saint-Etienne, France

[4] Université de Lyon, F-42023, Saint-Etienne, France

[5] CHU de Saint-Etienne, F-42055, Saint-Etienne, France

[6] Inserm U955, Equipe 10, Université Paris Est Créteil (UPEC), France

[7] Université Jean Monnet, Centre de Microscopie Confocale Multiphotonique, Pôle Optique et Vision, F-42023, Saint-Etienne, France

[8] Ecole Nationale Supérieure des Mines, CIS-EMSE, LINA EA 4624, F-42023, Saint-Etienne, France

Corresponding author: Dr Jean-Philippe Klein, Université Jean Monnet, Faculté de Médecine, F-42023 Saint-Etienne, France. Email: jeanphiklein@hotmail.fr. Phone number: + 33 4 77 82 83 07. Fax number: + 33 4 77 82 87 84

Abstract: The significant expansion in the use of nanoparticles and submicron particles during the last 20 years has led to increasing concern about their potential toxicity to humans and particularly their impact on male fertility. Currently, an insufficient number of studies have focused on the testicular biodistribution of particles. The aim of our study was to assess the distribution of 450 nm fluorescent particles in mouse testes after intramuscular injection. To this end, testes were removed from 5 groups of 3 mice each at 1 h (H1), 4 days (D4), 21 days (D21), 45 days (D45) and 90 days (D90) after the injection of 7.28×10^9 particles in the tibialis anterior muscles of each mouse. We examined histological sections from these samples by epifluorescence microscopy and confocal microscopy and identified testicular biodistribution of a small number of particles in groups H1, D4, D21, D45 and D90. Using CD11b immunostaining, we showed that particles were not carried into the testis by macrophages. The intratesticular repartition of particles mainly followed testicular vascularization. Finally, we found some particles in seminiferous tubules but could not determine if the blood–testis barrier was crossed.

Keywords: submicron particles, mice, testis, tissue distribution, intramuscular injections, macrophages

1 Introduction

Humans have always been exposed to nanoparticles and submicron particles in the environment through volcanic eruptions, forest fires or sand dust; however, environmental exposure has increased in recent history due to industrial activities and car pollution (Gaffet 2011). Moreover, during the last 20 years we have witnessed the emergence of nanotechnologies that have already found many applications in a wide variety of fields, such as textile industry, informatics, cosmetic or medicine. These new developments have led to increased exposure to engineered nanoparticles and nanomaterials. Nanoparticles have specific abilities to interact with biological structures mainly due to their small size and their high surface to volume ratio (Oberdörster et al. 1994). Thus, concerns about nanoparticle toxicity have been raised in the scientific community, and many studies have been done to assess the impact of nanoparticles on the environment and human health (Peralta-Videa et al. 2011)

Numerous pollutants, such as phthalate esters (Lucas et al. 2009), pesticides (Colborn et al. 2007) and bisphenol A (Chitra et al. 2003) may have an impact on human reproduction. Since nanoparticles can pass through biological membranes, especially the blood–air barrier (Nemmar et al. 2001; Oberdörster et al. 2002), or are directly injected into the blood circulation in some medical procedures, including new treatments for cancer (Schwartz et al. 2009) and for biomedical imaging (Bruns et al. 2009), fears have been raised about their ability to impair human reproduction, especially male fertility (Ema et al. 2010; Lan et al. 2012)

At this time few studies have focused on this topic. Due to a lack of standardization, it is quite difficult to draw conclusions, with some studies even leading to contradictory results. Two types of investigation were carried out in the studies reported in literature: a

determination of the biodistribution of nanoparticles in the testis and an assessment of the toxicity of nanoparticles on testicular cells.

Testicular biodistribution of nanoparticles has only been only studied in rodent models (Bai et al. 2010; Balasubramanian et al. 2010; De Jong et al. 2008; Kim et al. 2006; Kwon et al. 2008; Lankveld et al. 2010; Park et al. 2010). Although animals (mice and rats), exposure routes (intravenous, intraperitoneal, oral or respiratory) and physico-chemical properties of nanoparticles (silica, gold nanoparticles, silver nanoparticles and carbon nanotubes with a size between 10 and 323 nm) have differed, all studies have concluded that nanoparticles are able to reach the testis.

Testicular toxicity has been investigated using cell lines or animal models. In a spermatogonial stem cell model (C18-4), it was shown that regardless of the cell viability marker considered (mitochondrial function, lactate dehydrogenase leakage, apoptosis or necrosis assay), the nanoparticle form of an element (silver, molybdenum and aluminum) is more toxic than the soluble form (silver carbonate, sodium molybdate and aluminum chloride) (Braydich-Stolle et al. 2005). In a Leydig cell model (TM3) another study concluded that nanoparticles can affect steroidogenesis through the overexpression of some genes such as the steroidogenic acute regulatory gene (*StAR*) (Komatsu et al. 2008). In another study, 200 nm titanium dioxide particles increased mouse testis cell proliferation while silver nanoparticles appeared to be rather cytostatic as well as cytotoxic (Asare et al. 2012). In human spermatozoa, two studies found contradictory results, the first one showed that nanoparticles had no effect on the ability of spermatozoa to initiate acrosomic reaction and did not affect their motility (Ben-David Makhluf et al. 2006), while the second one found that gold nanoparticles lowered spermatozoon motility (Wiwanitkit et al. 2009). However, the latter study had some biases and is hard to interpret. In mice, intratracheally administered carbon black nanoparticles seem to impair spermatogenesis while increasing testosterone synthesis

(Yoshida et al. 2009). Additionally, repeated intravenous injections of carbon nanotubes in mice caused testicular damage that was reversible after injections were discontinued and did not affect fertility (Bai et al. 2010). In rats, inhalation of a specific amount of diesel exhaust nanoparticles disrupted the endocrine activity of the male reproductive system by increasing plasma and testicular testosterone and inhibin levels (Li et al. 2009). This could be explained by increased expression of StAR protein and P450 cytochrome (Ramdhan et al. 2009)

Since nanoparticles and submicron particles are increasingly used in medicine, especially as a vaccine adjuvant (Oyewumi et al. 2010; Singh et al. 2007; Peek et al. 2008), the aims of our study were to test whether particles could reach the testis following an intramuscular injection in a murine model and, if so, to track them inside the testis. Because macrophages are known to incorporate foreign bodies through phagocytosis and carry them towards various organs, we used fluorescent macrophage immunostaining to investigate whether macrophages could carry particles towards the testis. In order to observe individual particles with epifluorescence microscopy, we chose 450 nm fluorescent particles. Although this size exceeds the usual size of nanoparticles, which is less than 100 nm (Handy et al. 2008), it still accords with the size of medical substances that are injected by the intramuscular route such as vaccine adjuvants (Oyewumi et al. 2010; Singh et al. 2007; Peek et al. 2008)

2 Materials and Methods

2.1 Animals

Nineteen male C57BL6 mice (Centre d'Elevage René Janvier, France) were bred at the animal house of the Créteil Medicine University and used according to French law. Experiments were started between 6 and 8 weeks of age.

2.2 Particles

We used Fluoresbrite® Polychromated Red Microspheres provided by Polysciences, Inc. (France). Their maximal excitation wavelength is 529 nm, while their maximal emission wavelength is 546 nm. The original concentration was 3.64×10^{11} particles/mL. Particles

were characterized using scanning electron microscopy

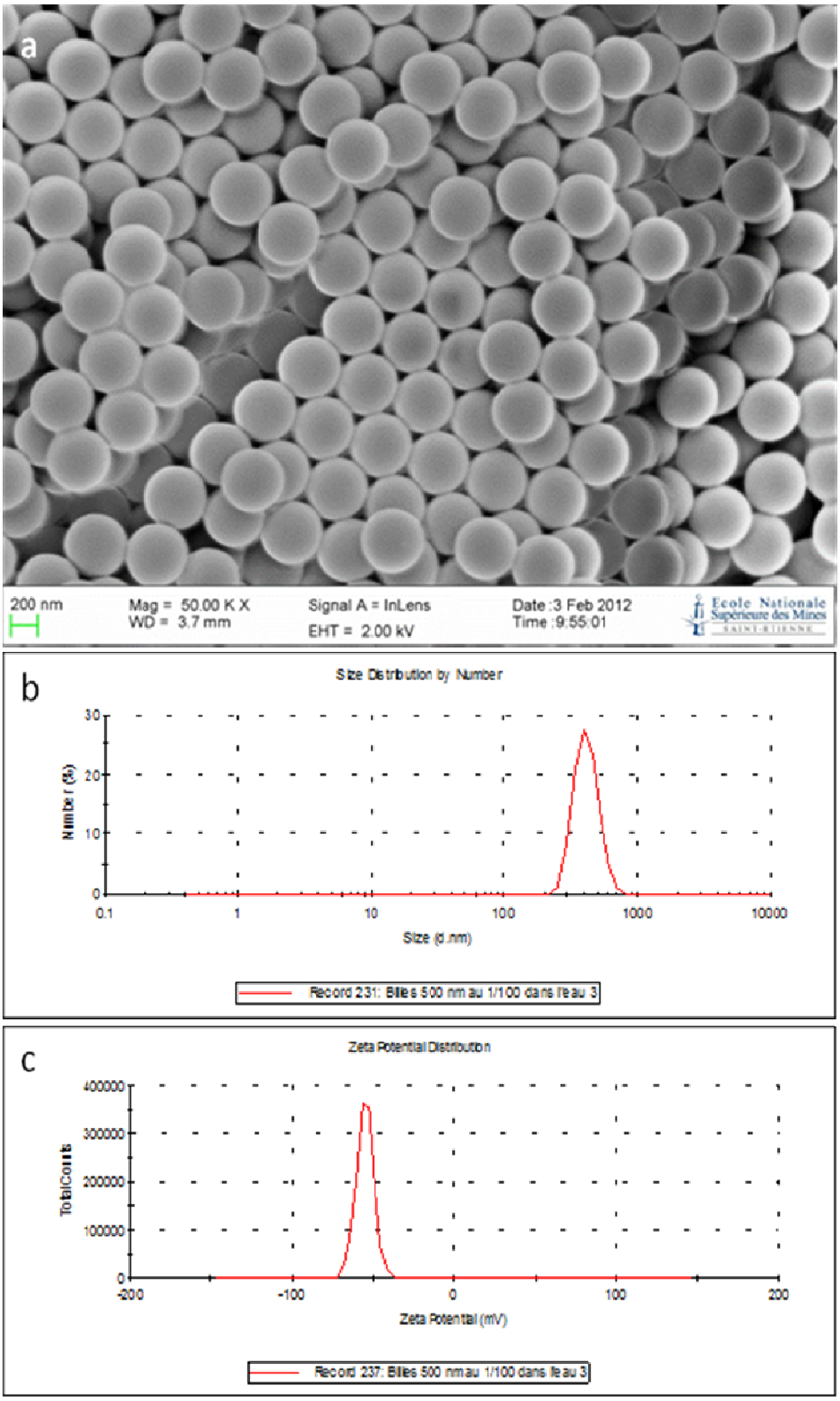

(

Fig. 1a) and photon correlation spectroscopy

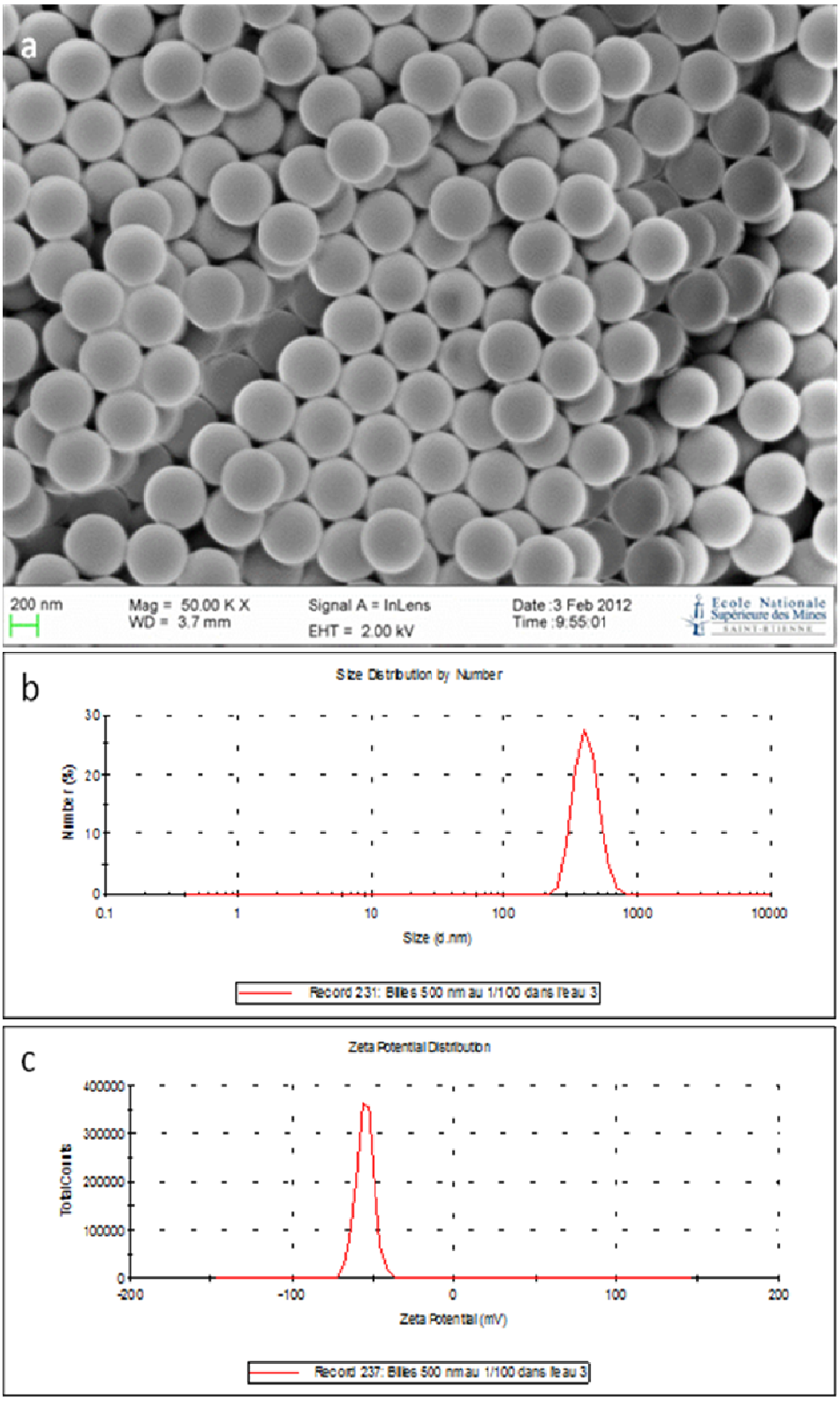

(

Fig. 1b and 1c). Particle size was approximately 450 nm with very few variations. No particle agglomeration was observed. Particle zeta potential was around −50 mV.

2.3 Intramuscular injection of particles

Particles were diluted 1:2 in phosphate-buffered saline (PBS), and 20 µL of the diluted particles was injected in each tibialis anterior muscle of 15 mice, for a total amount of 7.28×10^9 particles per mouse. Four other mice were injected with PBS alone as a negative control group.

2.4 Blood and testicular samples

The 15 mice that were injected with particles were divided into 5 groups that were sacrificed at 1 h (H1), 4 days (D4), 21 days (D21), 45 days (D45) or 90 days (D90) after the injection. Control group mice were sacrificed after 1 h. Mice were first anesthetized with a lethal dose of sodium pentobarbital (120 mg/kg, Ceva Sante Animal SA, France). The chest was then opened, 100 µL of blood was sampled from the right ventricle and spread on several glass slides. The bloodstream was perfused with PBS and tissues were fixed with a 4% paraformaldehyde (PFA) solution. Once the first fixation was done, testes were excised and fixed in a 4% PFA solution for 4 h, after which they were cryoprotected in a 30% sucrose solution for 24 h. After being coated in a cryopreservative solution (Tissue-Tech®: Sakura, Netherlands), testes were frozen in liquid nitrogen (−196°C) and stored at −80°C

2.5 Histological slide preparation

Each slide (Superfrost Plus®: Thermo Scientific) was wiped with an alcohol swab to remove any dust that could cause unwanted fluorescence. Eleven 10-µm-thick sections were cut from one testis of each mouse with a microtome (Leica CM 3000®). Sections were not adjacent and have been cut from different part of the testis. As mouse testis is a homogenous organ, it was assessed that each section was representative of the whole testis. One section was stained with toluidine blue in order to assess preservation of the testes. Five sections were dried and

mounted with an appropriate mounting medium (Fluokeep®: Argene, France) and the five remaining sections were immunostained. Once mounted, slides were stored at 4°C in the dark.

2.6 Macrophage staining

Anti-CD11b antibody specifically labels the plasma membrane of macrophages. To determine if nanoparticles were carried to testis by macrophages or were free in the testicular stroma, we performed an indirect immunofluorescence procedure using a specific monoclonal rat anti-mouse anti-CD11b antibody (clone 5C6, Adb Serotec, United Kingdom). First, slides were washed in PBS containing 0.5% Triton X-100 (PBST) for 5 min and pre-incubated in a blocking solution of PBST containing 3% bovine serum albumin for 15 min. Slides were then incubated for 1 h in a humid chamber with the anti-CD11b primary antibody diluted 1:200 in antibody diluent (Dako, France). After rinsing in PBST and then PBS, slides were incubated for 30 min with a polyclonal goat anti-rat secondary antibody (Adb Serotec, United Kingdom) conjugated with green fluorescent dyes (Dylight® 488) and diluted 1:200. Finally, they were rinsed in PBST, PBS and pure water one last time before application of Fluokeep medium and storage at 4°C in a dark place until analysis.

2.7 Epifluorescence microscopy and confocal microscopy

Slides were observed using an epifluorescence microscope (motorized Olympus Ix81) to detect particles (excitation: 554 nm, emission: 568 nm) and to analyze CD11b labeling (excitation: 490 nm, emission: 520 nm). In order to differentiate particles from fluorescent dust or from free dyes, we compared their aspect with a sprawl of isolated microspheres and defined several morphological criteria such as an appropriate size and a spherical shape. Autofluorescence in the testis was a major issue throughout the study, and it made particle observations particularly difficult. To ensure that observed particles were really the injected submicron particles and not autofluorescence, confocal microscopy was performed to establish the emission spectra of autofluorescent areas of the testis compared with pure

submicron particles. To that purpose, both the autofluorescent areas and the particles were excited at 800 nm, and fluorescence was then measured between 350 nm and 840 nm. A comparison of the different emission spectra allowed us to distinguish injected particles from autofluorescence.

3 Results

3.1 Preservation of testes

Analysis of slides stained with toluidine blue showed that testicular morphology was well preserved (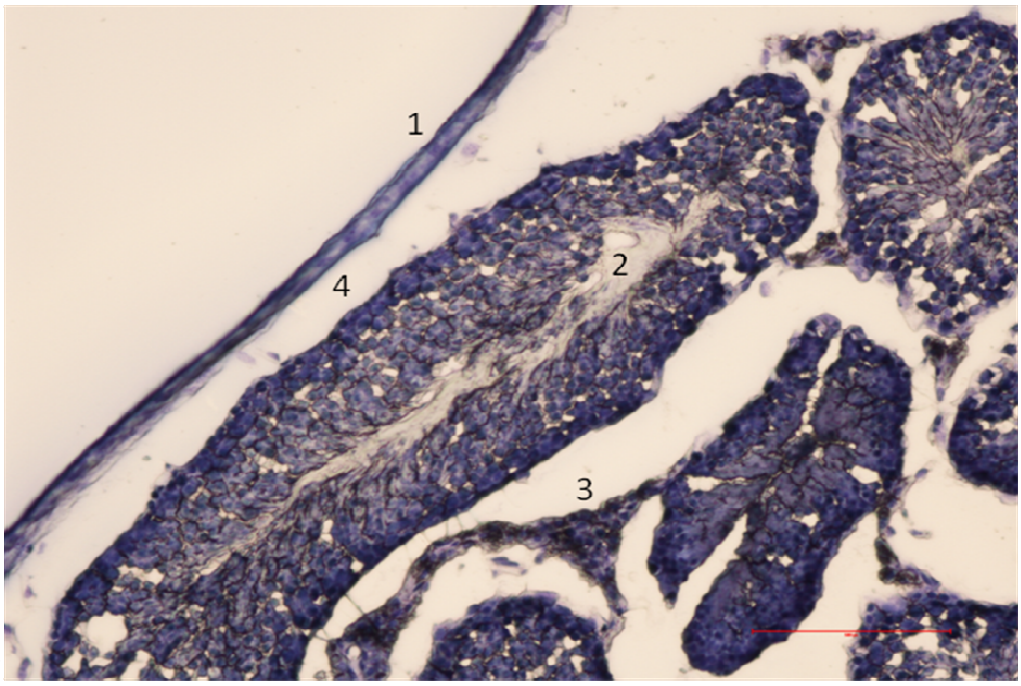

Fig. 2).

3.2 Blood Analysis

Fluorescent submicron particles were observed on blood smears at each survival time analyzed, with a maximum at D21

(

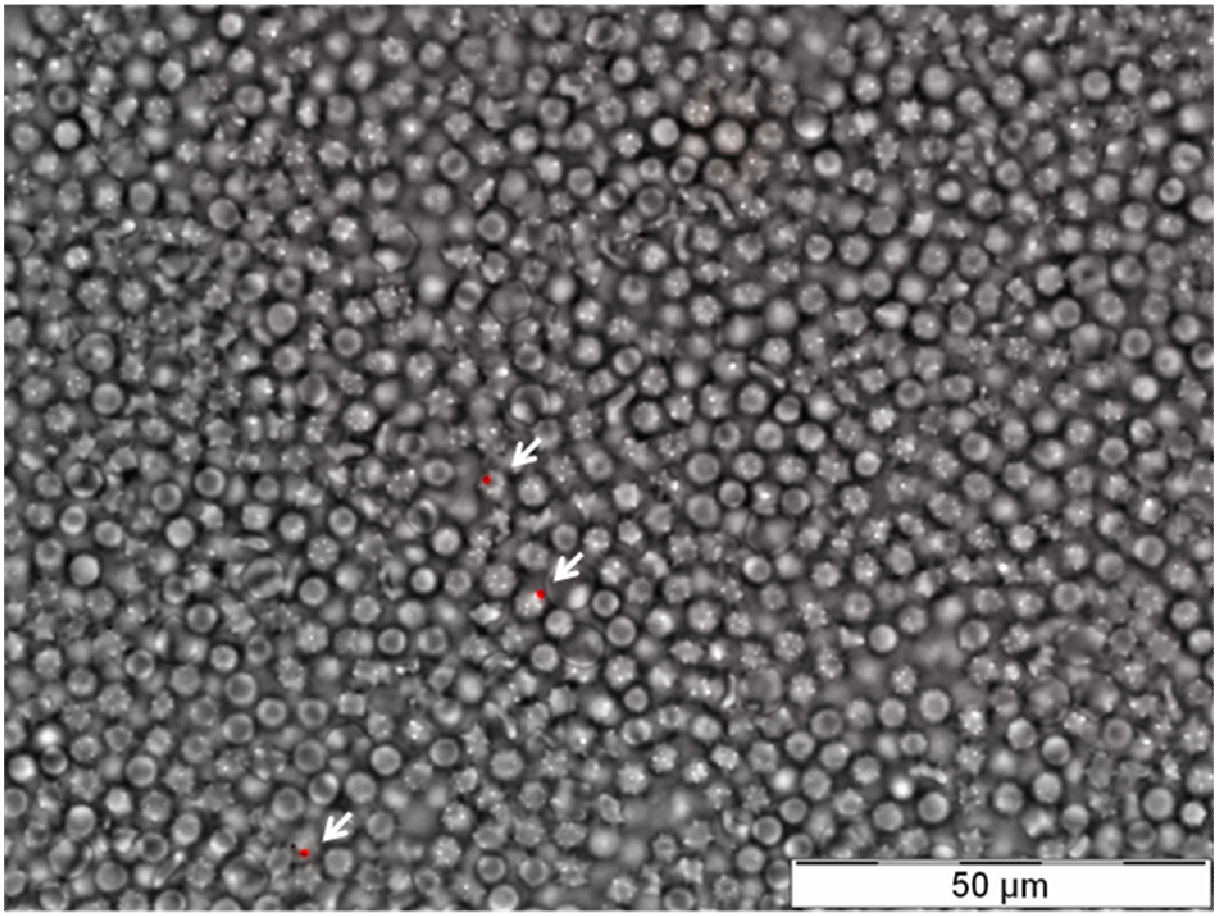

Fig. 3).

3.3 Testicular autofluorescence

The first finding in the epifluorescence analysis of the testicular sections was the presence of significant autofluorescence

(

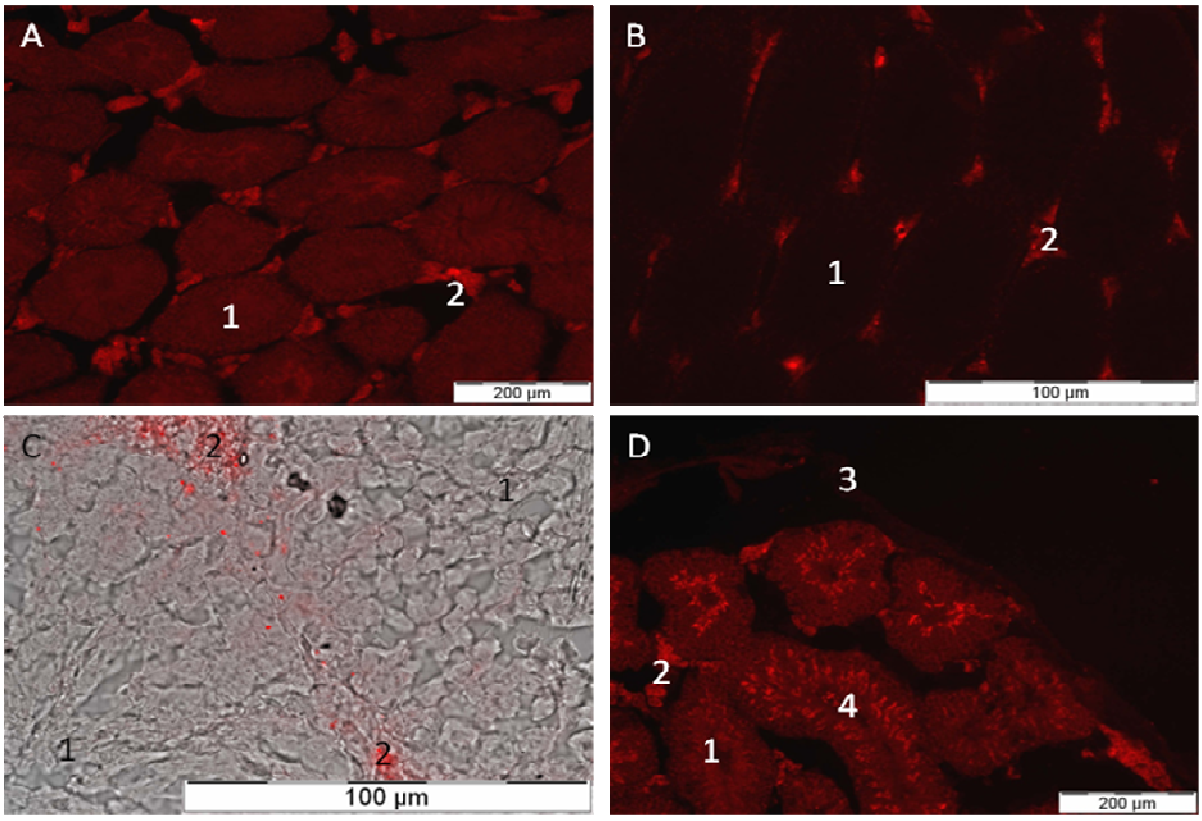
A
1
2
200 µm
B
1
2
100 µm
C
2
1
1
2
100 µm
D
3
2
4
1
200 µm

Fig. 4a). It was particularly intense in the intertubular compartment where Leydig cells lie (

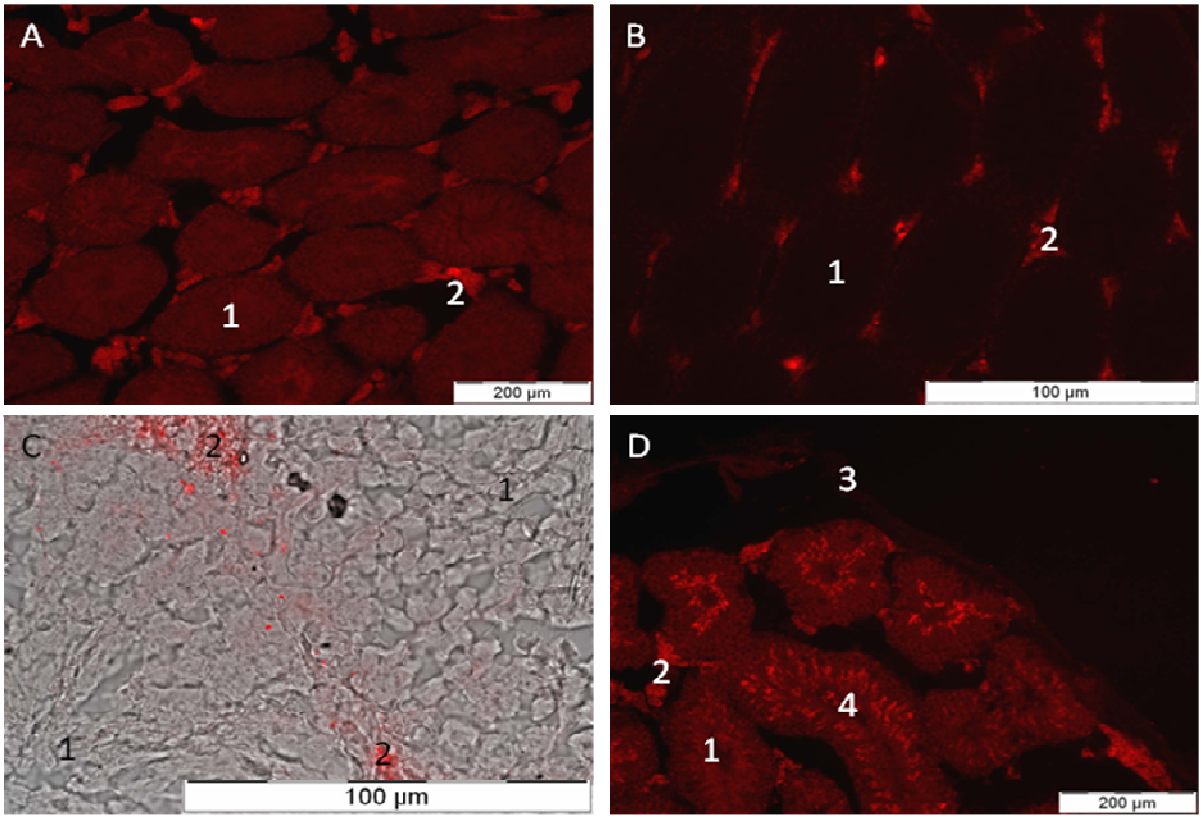

Fig. 4b). Interstitial autofluorescence sometimes hardly differed from the particles' fluorescence

(

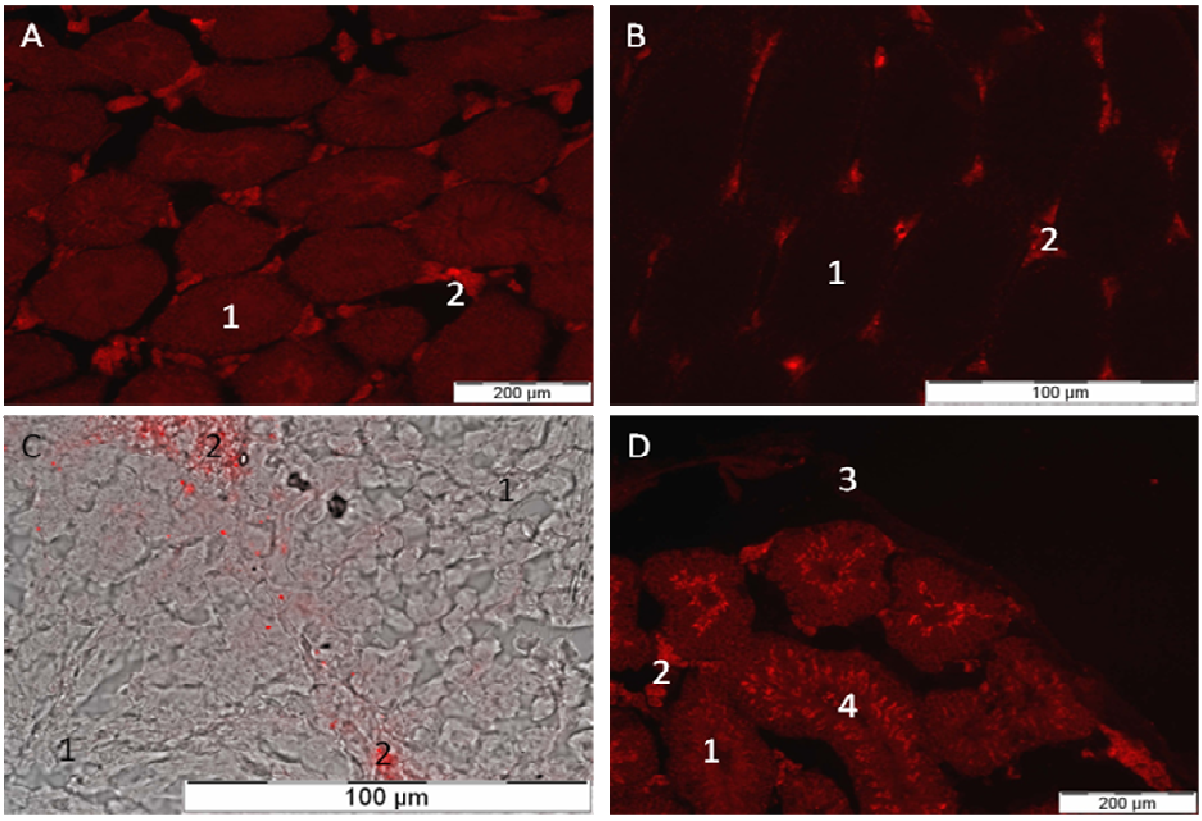

Fig. 4c). Although tubular autofluorescence was less pronounced, some of the seminiferous tubules showed intense adluminal fluorescence

(

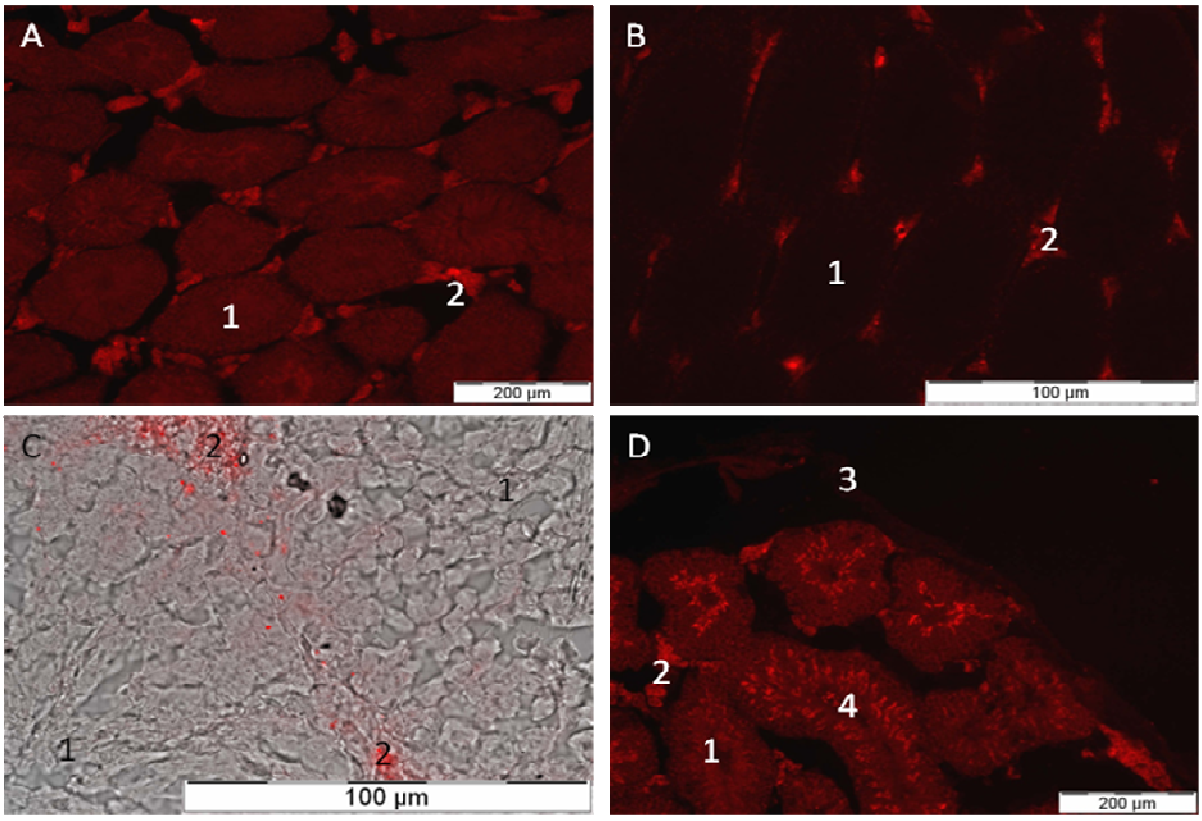

Fig. 4d). We found that this autofluorescence was emitted by spermatozoa heads at the end of spermatogenesis.

3.4 Particle biodistribution

Up to 190 sections were thoroughly analyzed, 40 sections from the control group and 30 sections from each of the other groups. All slides considered, 50 particles were found. No particles were found in the control group, 22 were found in the H1 group, 5 in the D4 group, 6 in the D21 group, 14 in the D45 and only 3 in the D90 group (Table 1).

Using morphological analysis, we were able to differentiate four histological compartments: the tunica albuginea, sub-albuginea spaces, interstitial spaces and seminiferous tubules (

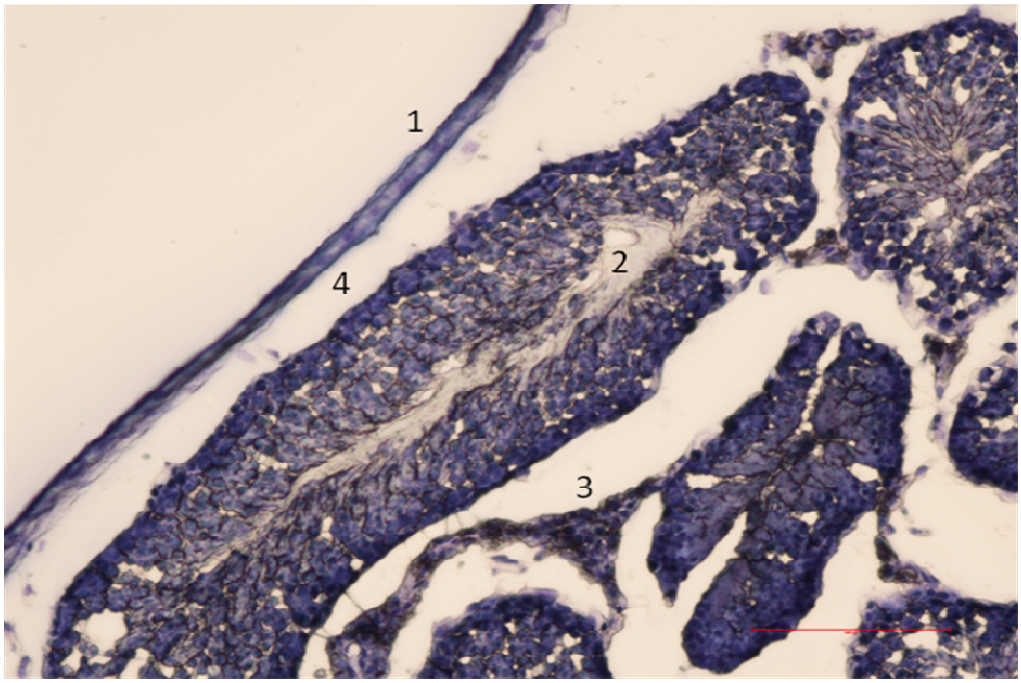

Fig. 2). Twenty-three particles were located in the tunica albuginea (

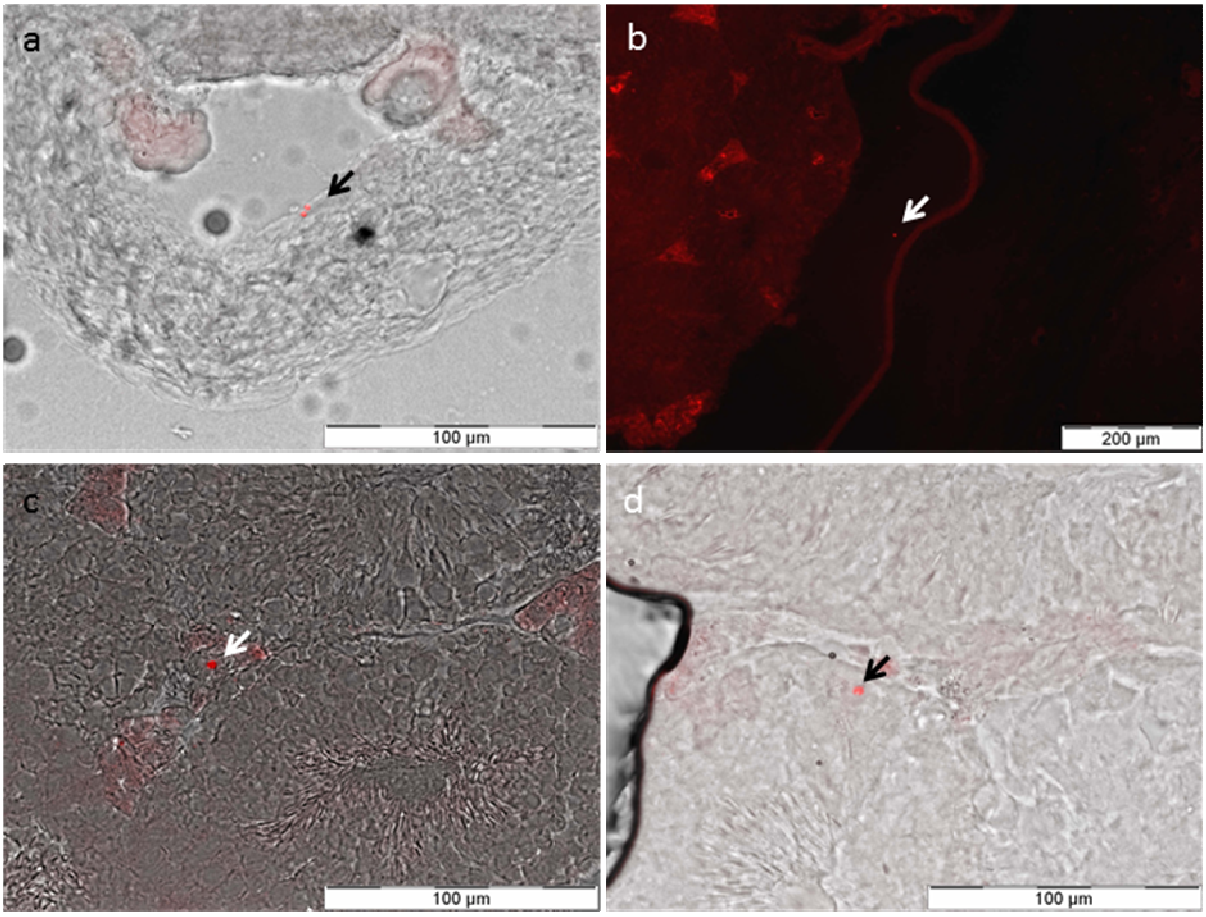

Fig. 5a) or in sub-albuginea spaces

(

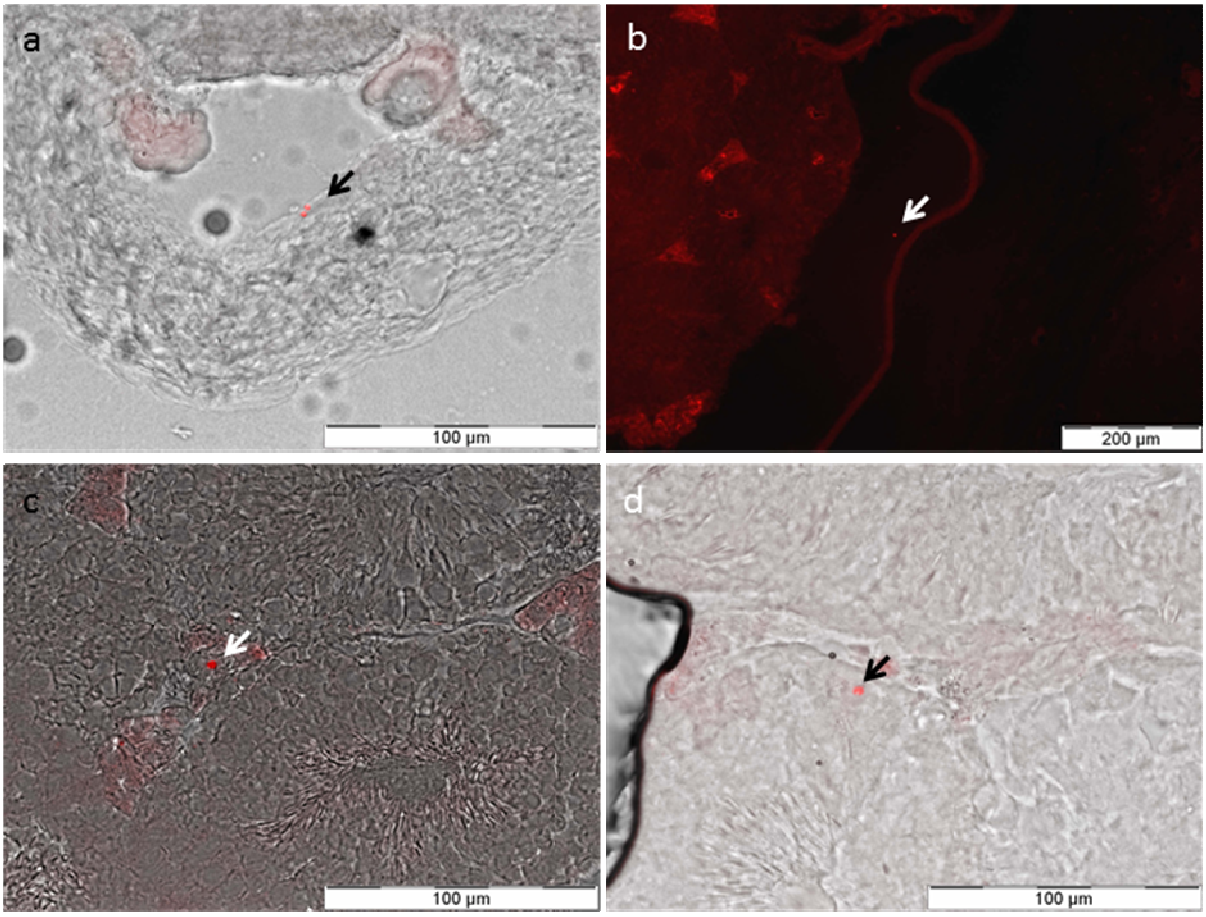

Fig. 5b), 15 particles in interstitial spaces
(

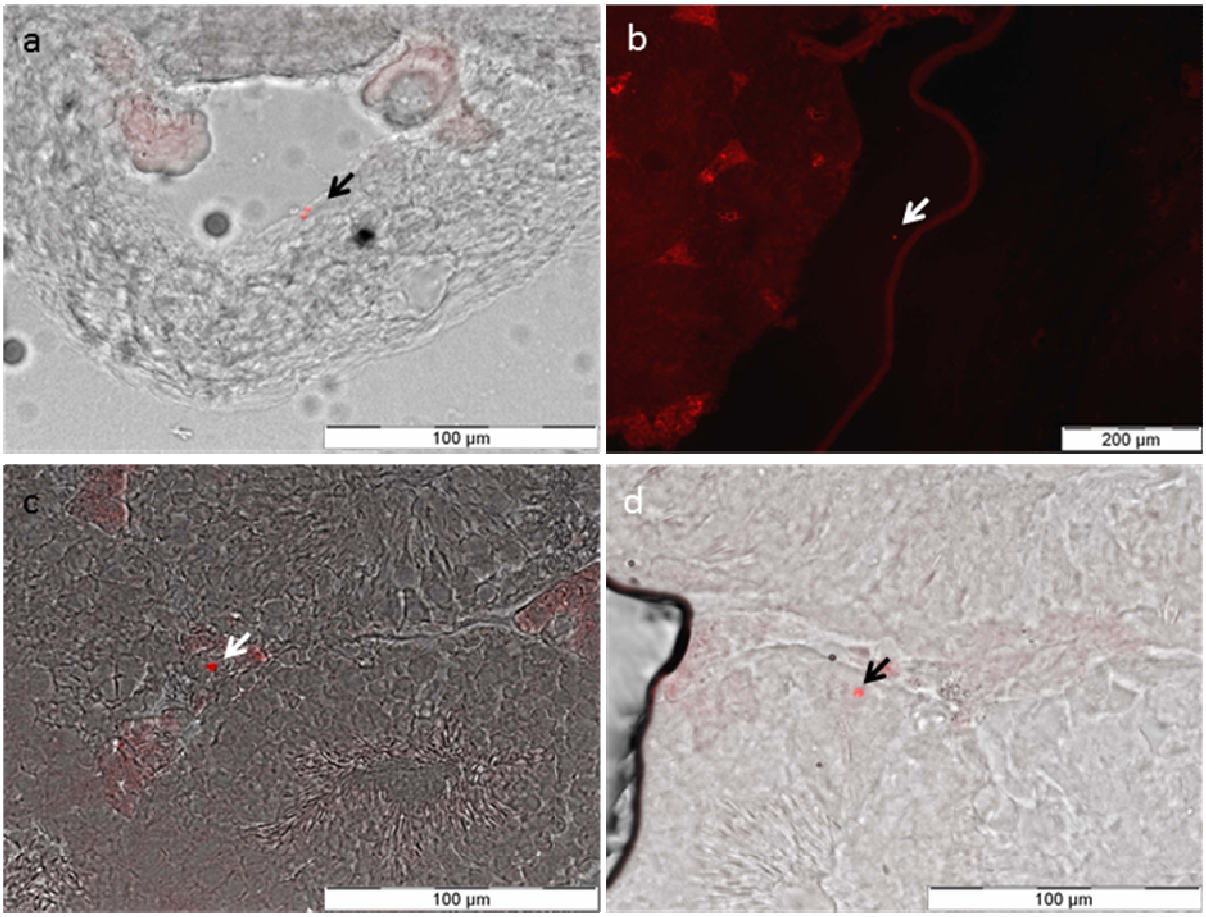

Fig. 5c) and 8 in seminiferous tubules (

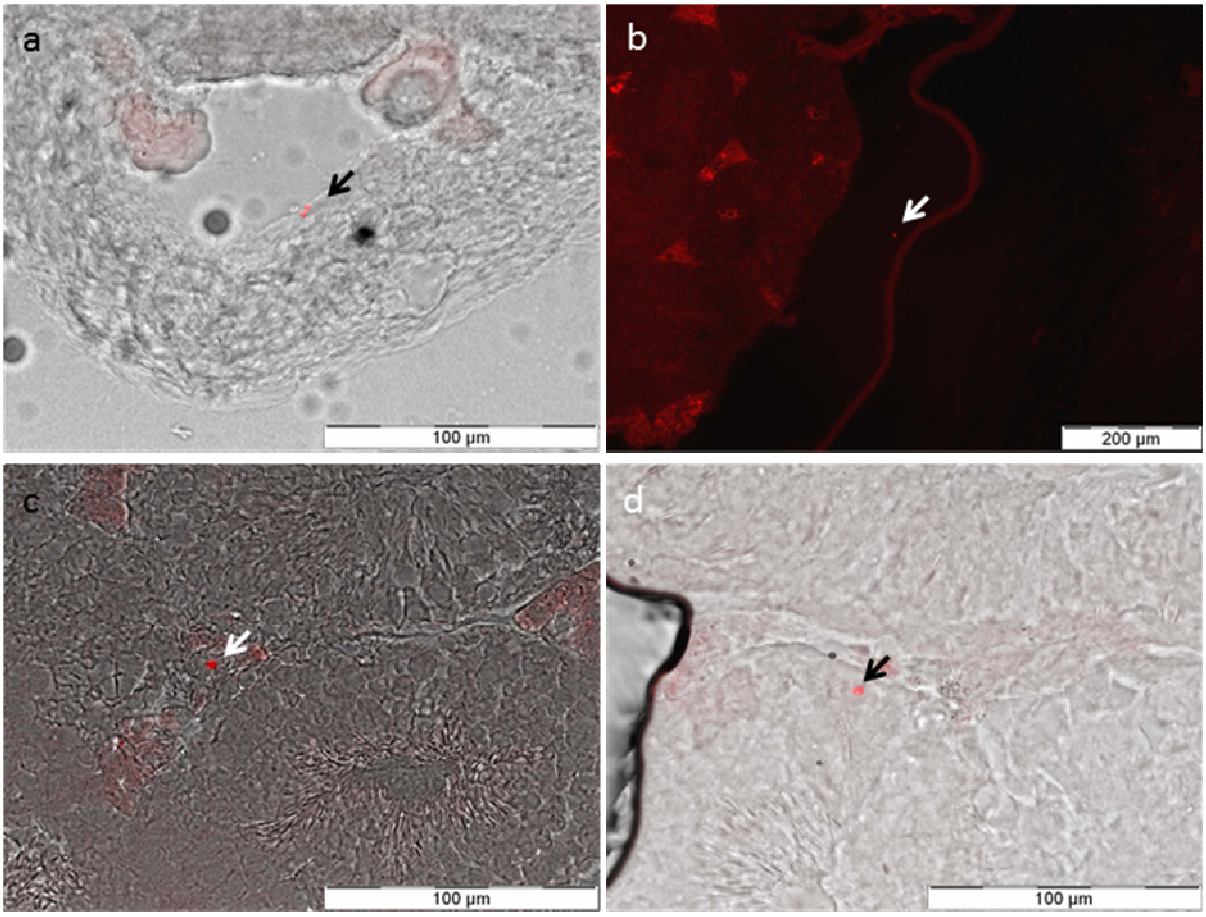

Fig. 5d). Due to poor section quality, we were not able to precisely localize 4 of the 50 particles

Intra-testicular particle distribution analysis based on the time post-injection revealed that H1 and D4 particles were more likely to be located in the tunica albuginea, while their distribution was more uniform at later time points. In particular, some particles were located in seminiferous tubules at D21 and D45.

3.5 Macrophage staining

Twenty-two particles were found in the testicular sections stained with the anti-CD11b antibody (Table 2). Among them, 15 were found to be distant from macrophages (

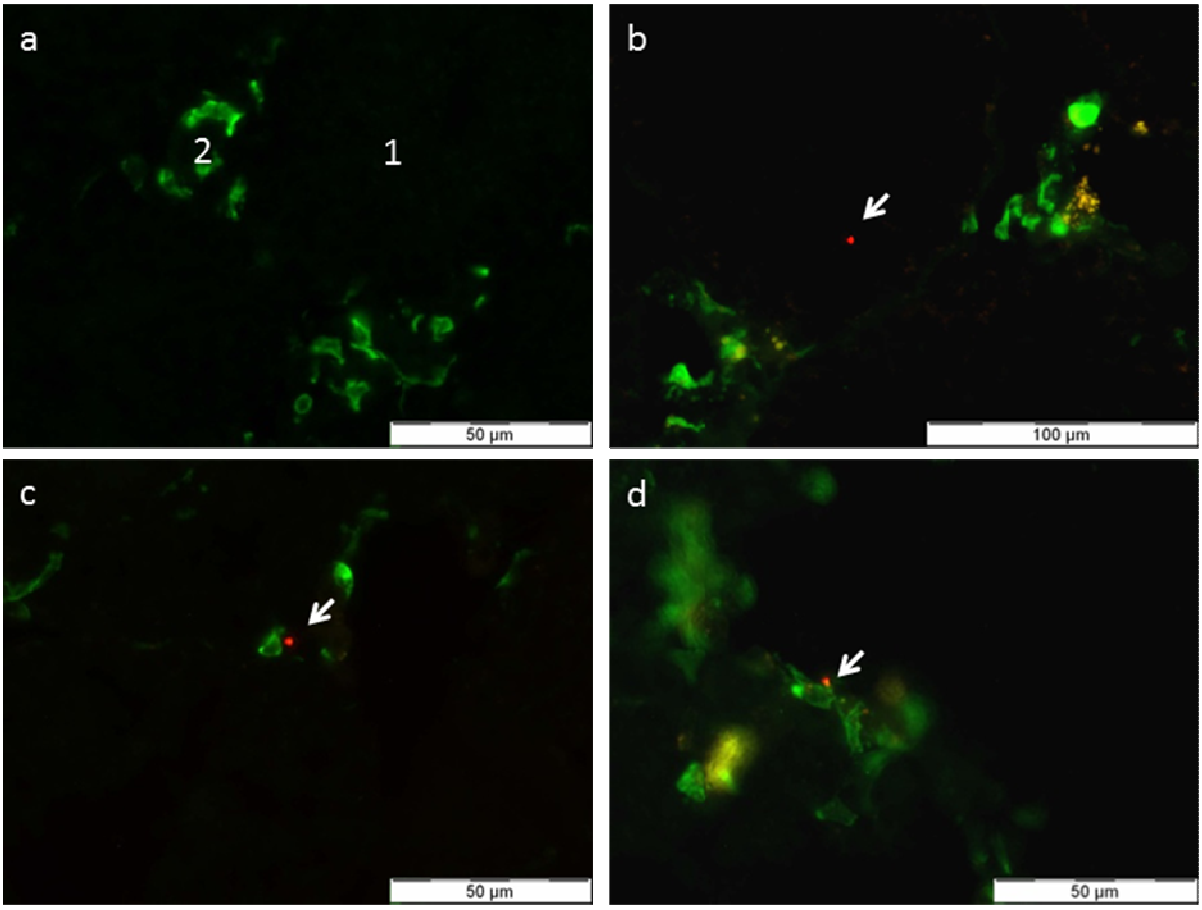

Fig. 6b and 6c) while 7 were in contact with macrophages (

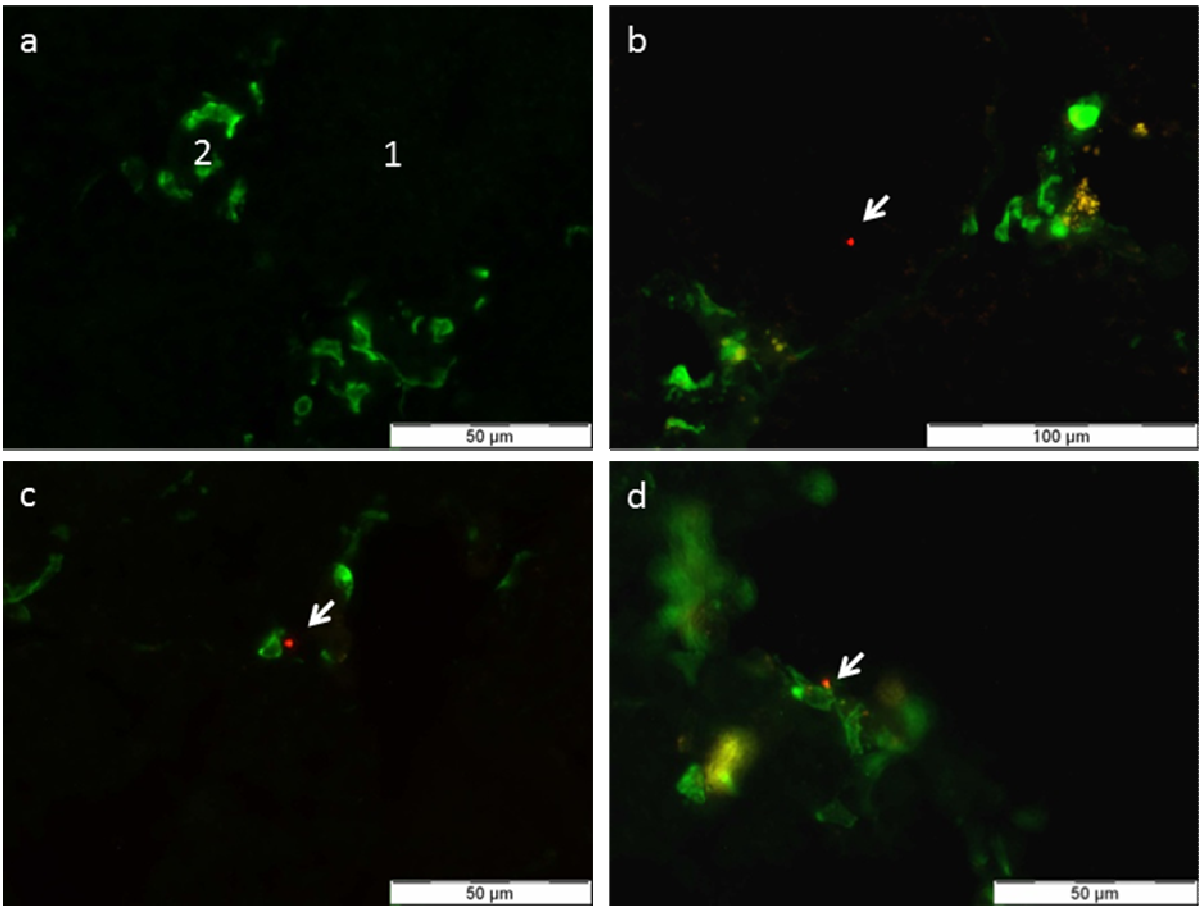

Fig. 6d). No particle seemed to be internalized by macrophages (particles and CD11B staining colocalization). These observations were irrespective of the time of analysis. Indeed, particles that reached the testis were mainly free, even at late time points after the injection.

3.6 Emission spectra analysis

In order to distinguish fluorescent submicron particles from testicular autofluorescence, their emission spectra were established using confocal microscopy. We found that autofluorescent

tissues had a small and wide emission peak between 460 nm and 710 nm

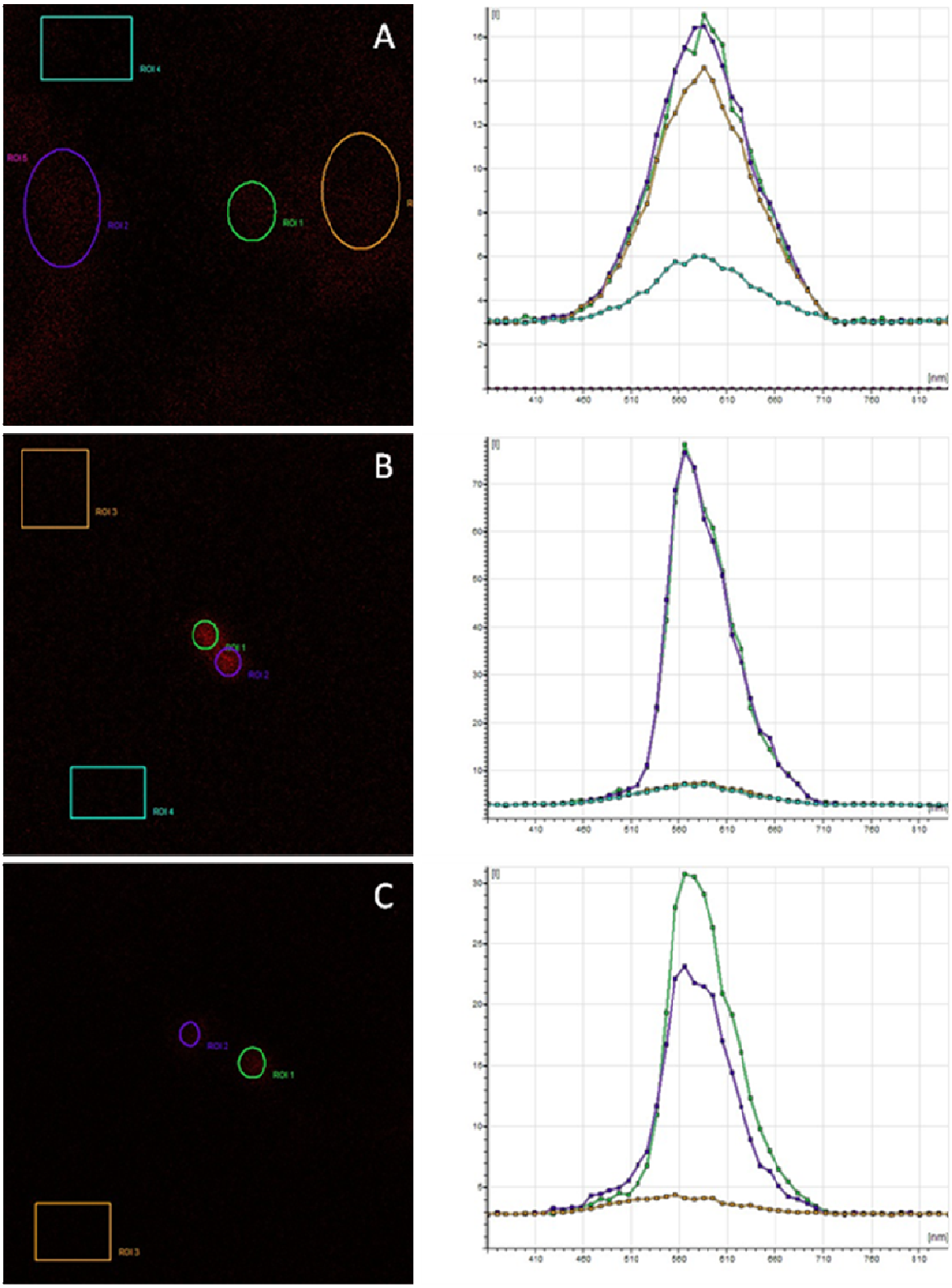

(

Fig. 7a), while submicron particles exhibited a higher and thinner emission peak between 520 nm and 690 nm

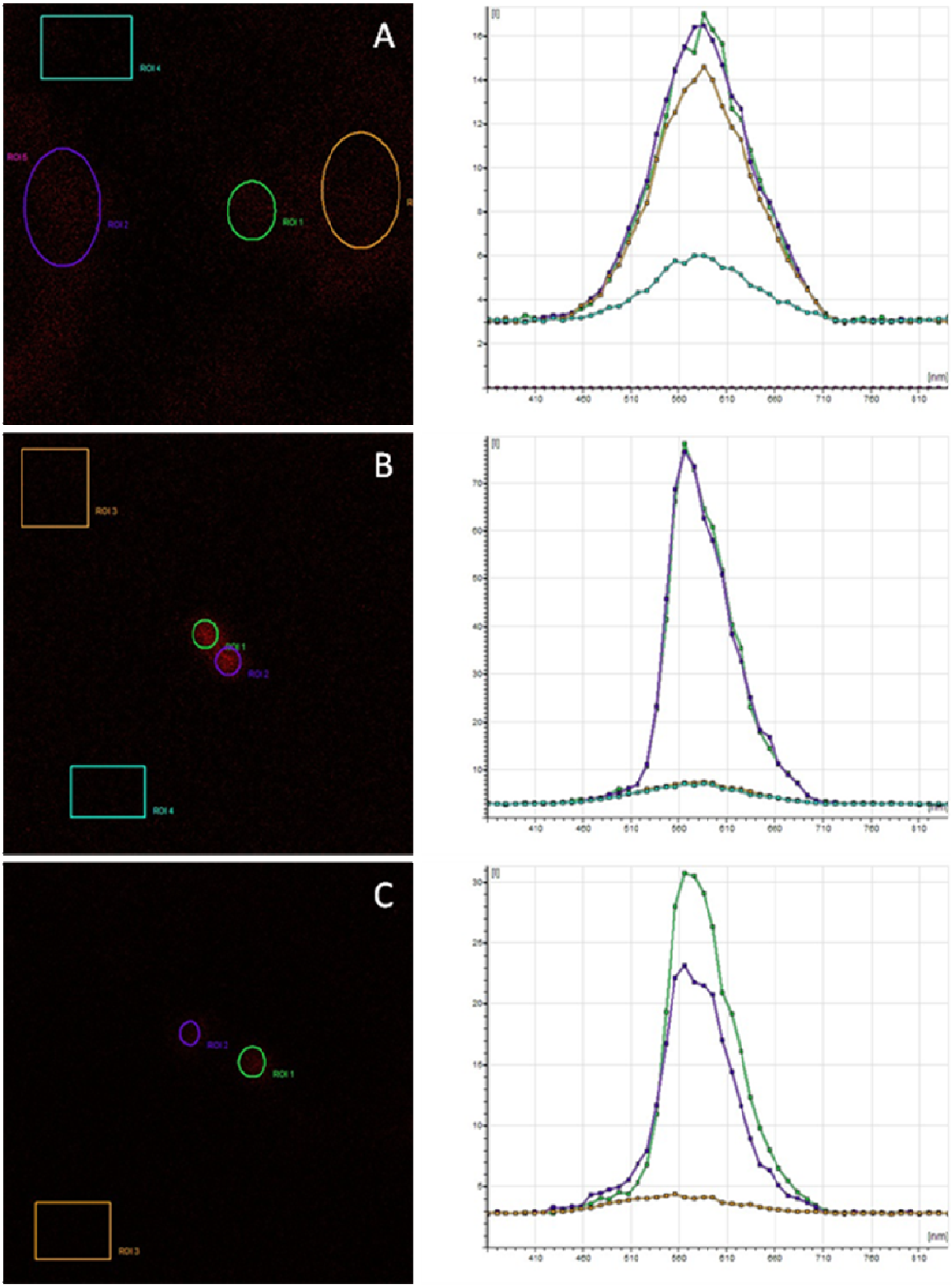

(

Fig. 7b). Eventually, the emission spectrum of particles found in mouse testes was the same as control submicron particles

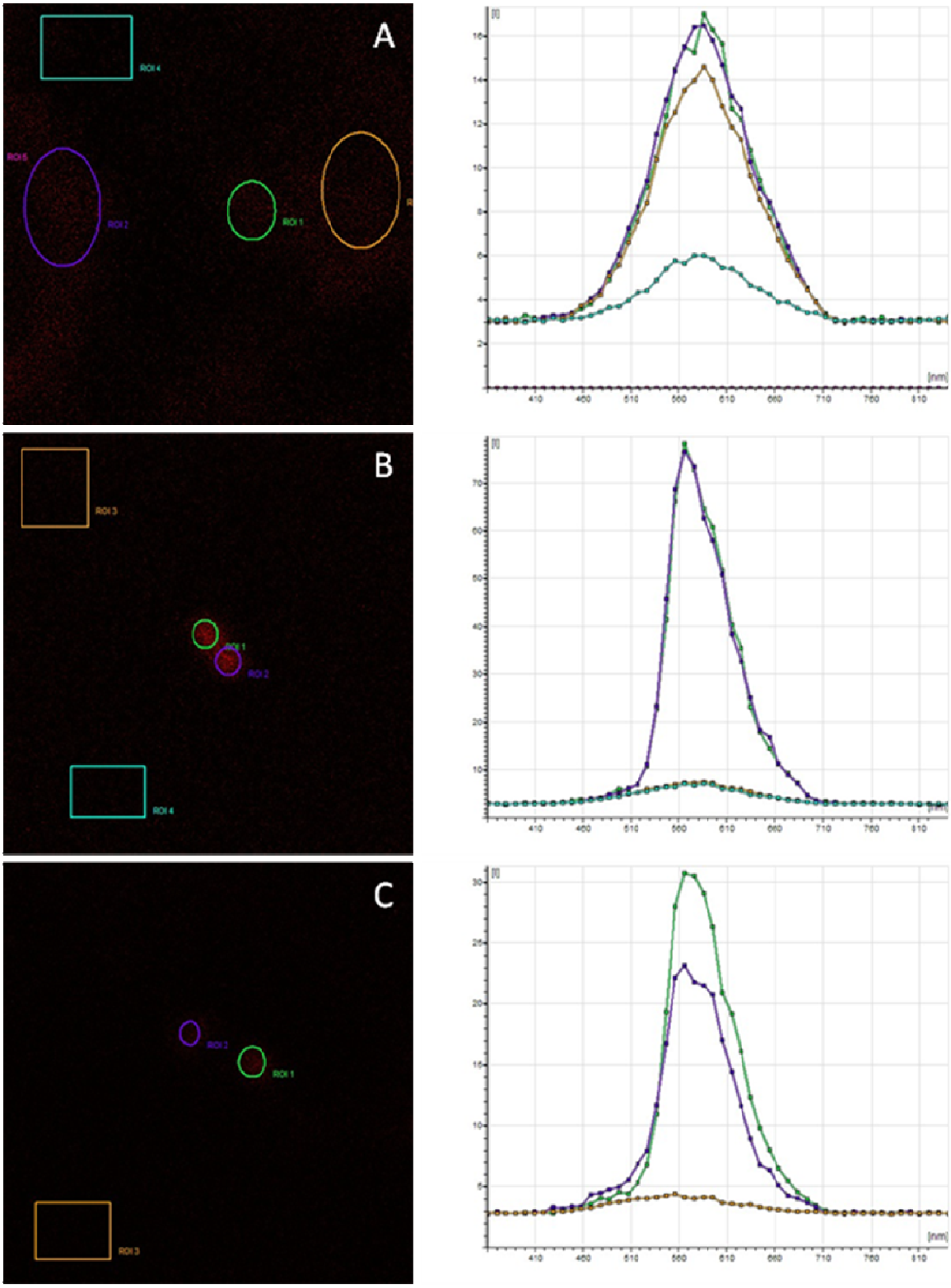

(

Fig. 7c), thus we were able to conclude with confidence that observed particles were the injected submicron particles and not an autofluorescent artifact.

4 Discussion

In this study we chose to use submicron particles rather than ones that were strictly nanoparticles. Since microscopy is the only way to study intratesticular biodistribution of particles and since the maximal resolution of optical microscopy is 200 nm (Hell et al. 2004), the use of larger particles was legitimate. Moreover, larger particles allowed us to track single particle uptake inside cells when only one particle was included.

The aim of our study was first to assess if intramuscularly injected nanoparticles were able to reach the testis through blood circulation. We demonstrated not only that 450 nm particles could translocate from muscles to blood circulation but also that a small amount of them could reach the testes. This result appears to conflict with findings by De Jong et al. (2008) which showed that only particles smaller than 50 nm could reach the testis. Differences between animal models, injection routes or nanoparticle structures could explain these divergent results, and another reason could be a lack of sensitivity of the inductively coupled plasma and mass spectroscopy (ICP-MS) used in their study. They were able to detect particles from 10^4 particles per gram of organ, while we were able to observe individual particles. The aim of our study was not to quantify the number of particles that were able to reach testis. Indeed we only observed a small part of each testis as fluorescent microscopy is not well suited to study whole testes from several mice. However, we found that there were very few particles in the testes; even if we slightly underestimated it due to the technique we performed, such a small number would be undetectable by ICP-MS. Finally, our findings match the results described by De Jong et al. (2008), Lankveld et al (2010) and Balabrasumian et al. (2010).

However, our results completely conflict with those of Kim et al. (2006) and Kwon et al. (2008). In these two studies, led by the same research group, it was shown in a mouse model that fluorescent 50 nm nanoparticles strongly migrate to the testis by both injection and inhalation routes. Kim et al. (2006) even suggested that particles could cross the blood–testis barrier based on the observation of adluminal fluorescence. Even if these discrepancies could be explained by the smaller size of their particles, it would be interesting to have the spectra analysis of the fluorescence they observed as we previously saw that the testis shows an intense autofluorescence in intertubular spaces and in the adluminal part of seminiferous tubules. Moreover, particles used in those studies had a smaller size than the resolution of an optical microscope which is around 200 nm (Hell et al. 2004). Thus, in these experimental conditions, it seems it would be difficult to observe 50 nm individual particles and to distinguish them from testicular autofluorescence. In our study, we analyzed the emission spectra of particles and the testis in order to distinguish particles from testicular autofluorescence

Most of the particles were observed in the testis 1 h after injection. This means that some of the particles quickly left muscles to reach the blood circulation and, from there, to enter the testis. During the following days, only a few of particles stayed in the testis, while the others were most likely eliminated through blood circulation.

Our second objective was to determine intra-testicular distribution of the particles. While most of the testis is composed of seminiferous tubules, nearly half of the particles were found in albuginea or in sub-albuginea space and more than a quarter were found in interstitial spaces, especially soon after injection (H1, D4). This distribution is not surprising because it perfectly matches testicular vascularization. In fact, it shows that particles were carried towards the testis by the bloodstream. While some particles were found in the seminiferous

tubules, especially at later time points, it is impossible to conclude that particles crossed the blood–testis barrier without examination by electron microscopy.

Our third objective was to investigate the macrophages' ability to carry particles from muscle towards the testis. Our hypothesis was that macrophages could serve as "Trojan horses" for particles to enter the testis. As described in literature, macrophages are only found in interstitial spaces (Hume et al. 1984). However, no particles were found inside macrophages and only a few were even found close to macrophages. Moreover, the highest number of particles in the testis was observed 1 h after injection, when there were many free particles in the bloodstream. Although it is still possible that macrophages may have carried particles to the testis and unloaded them there, our observations do not confirm the Trojan horse hypothesis.

In conclusion, we have shown that 450 nm particles injected intramuscularly in a murine model can reach the testis through blood circulation in very small numbers, and they are probably not carried by macrophages. We also showed that intratesticular repartition of particles mainly follows testicular vascularization. We found some particles in seminiferous tubules without being able to determine if the blood–testis barrier was crossed. Thus, complementary studies, probably including the use of electron microscopy, are needed to answer to this question.

Acknowledgments

Special thanks to the members of the nephrology laboratory of Saint-Etienne north hospital, especially Brigitte Roman, for their help during slide production and to the members of the BIIGC laboratory, especially Zhiguo He, for their help with epifluorescence microscopic analysis.

References

N. Asare, C. Instanes, W.J. Sandberg, M. Refsnes, P. Schwarze, M. Kruszewski, G. Brunborg, Toxicology **291**, 65 (2012).

Y. Bai, Y. Zhang, J. Zhang, Q. Mu, W. Zhang, E.R. Butch, S.E. Snyder, B. Yan, Nat. Nanotechnol. **5**, 683 (2010).

S.K. Balasubramanian, J. Jittiwat, J. Manikandan, C.-N. Ong, L.E. Yu, W.-Y. Ong, Biomaterials **31**, 2034 (2010).

S. Ben-David Makhluf, R. Qasem, S. Rubinstein, A. Gedanken, H. Breitbart, Langmuir **22**, 9480 (2006).

L. Braydich-Stolle, S. Hussain, J.J. Schlager, M.-C. Hofmann, Toxicol. Sci. **88**, 412 (2005).

O.T. Bruns, H. Ittrich, K. Peldschus, M.G. Kaul, U.I. Tromsdorf, J. Lauterwasser, M.S. Nikolic, B. Mollwitz, M. Merkel, N.C. Bigall, S. Sapra, R. Reimer, H. Hohenberg, H. Weller, A. Eychmüller, G. Adam, U. Beisiegel, J. Heeren, Nat. Nanotechnol. **4**, 193 (2009).

K.C. Chitra, K.R. Rao, P.P. Mathur, Asian J. Androl. **5**, 203 (2003).

T. Colborn, L.E. Caroll, Hum. Ecol. Risk Assess. **13**, 1078 (2007).

M. Ema, N. Kobayashi, M. Naya, S. Hanai, J. Nakanishi, Reprod. Toxicol. **30**, 343 (2010).

E. Gaffet, Comptes Rendus - Physique **12**, 648 (2011).

R.D. Handy, F. Kammer, J.R. Lead, M. Hassellöv, R. Owen, M. Crane, Ecotoxicology **17**, 287 (2008).

S.W. Hell, M. Dyba, S. Jakobs, Curr. Opin. Neurobiol. **14**, 599 (2004).

D.A. Hume, D. Halpin, H. Charlton, S. Gordon, Proc. Natl. Acad. Sci. U.S.A **81**, 4174 (1984).

Wim H De Jong, W.I. Hagens, Petra Krystek, M.C. Burger, A.J.A.M. Sips, Robert E Geertsma, Biomaterials **29**, 1912 (2008).

J.S. Kim, T.-J. Yoon, K.N. Yu, B.G. Kim, S.J. Park, H.W. Kim, K.H. Lee, S.B. Park, J.-K. Lee, M.H. Cho, Toxicol. Sci. **89**, 338 (2006).

T. Komatsu, M. Tabata, M. Kubo-Irie, T. Shimizu, K.-I. Suzuki, Y. Nihei, Ken Takeda, Toxicol. In Vitro **22**, 1825 (2008).

J.-T. Kwon, S.-K. Hwang, H. Jin, D.-S. Kim, A. Minai-Tehrani, H.-J. Yoon, M. Choi, T.-J. Yoon, D.-Y. Han, Y.-W. Kang, B.-I. Yoon, J.-K. Lee, M.-H. Cho, J. Occup. Health **50**, 1 (2008).

Z. Lan, W.-X. Yang, Nanomedicine (Lond) **7**, 579 (2012).

D.P.K. Lankveld, A.G. Oomen, P Krystek, A. Neigh, A. Troost-de Jong, C.W. Noorlander, J.C.H. Van Eijkeren, R E Geertsma, W H De Jong, Biomaterials **31**, 8350 (2010).

C. Li, S. Taneda, K. Taya, G. Watanabe, X. Li, Y. Fujitani, Y. Ito, T. Nakajima, A.K. Suzuki, Inhal. Toxicol. **21**, 803 (2009).

B. Lucas, C. Fields, M.-C. Hofmann, Birth Defects Res. C Embryo Today **87**, 35 (2009).

A. Nemmar, H. Vanbilloen, M.F. Hoylaerts, P.H.M. Hoet, A. Verbruggen, B. Nemery, Am. J. Resp. Crit. Care Med. **164**, 1665 (2001).

G. Oberdörster, J. Ferin, B.E. Lehnert, Environ. Health Perspect. **102 Suppl 5**, 173 (1994).

G. Oberdörster, Z. Sharp, V. Atudorei, A. Elder, R. Gelein, A. Lunts, W. Kreyling, C. Cox, J. Toxicol. Environ. Health A **65**, 1531 (2002).

M.O. Oyewumi, A. Kumar, Z. Cui, Expert Rev. Vaccines **9**, 1095 (2010).

E.-J. Park, E. Bae, J. Yi, Y. Kim, K. Choi, S.H. Lee, J. Yoon, B.C. Lee, K. Park, Environ. Toxicol. Pharmacol. **30**, 162 (2010).

L.J. Peek, C.R. Middaugh, C. Berkland, Adv. Drug Deliv. Rev. **60**, 915 (2008).

J.R. Peralta-Videa, L. Zhao, M.L. Lopez-Moreno, G. de la Rosa, J. Hong, J.L. Gardea-Torresdey, J. Hazard. Mater. **186**, 1 (2011).

D.H. Ramdhan, Y. Ito, Y. Yanagiba, N. Yamagishi, Y. Hayashi, C. Li, S. Taneda, A.K. Suzuki, G. Watanabe, K. Taya, M. Kamijima, T. Nakajima, Toxicol. Lett. **191**, 103 (2009).

J.A. Schwartz, A.M. Shetty, R.E. Price, R.J. Stafford, J.C. Wang, R.K. Uthamanthil, K. Pham, R.J. McNichols, C.L. Coleman, J.D. Payne, Cancer Res. **69**, 1659 (2009).

M. Singh, A. Chakrapani, D. O'Hagan, Expert Rev. Vaccines **6**, 797 (2007).

V. Wiwanitkit, A. Sereemaspun, R. Rojanathanes, Fertil. Steril. **91**, e7 (2009).

S. Yoshida, K. Hiyoshi, T. Ichinose, H. Takano, S. Oshio, I. Sugawara, K Takeda, T. Shibamoto, Int. J. Androl. **32**, 337 (2009).

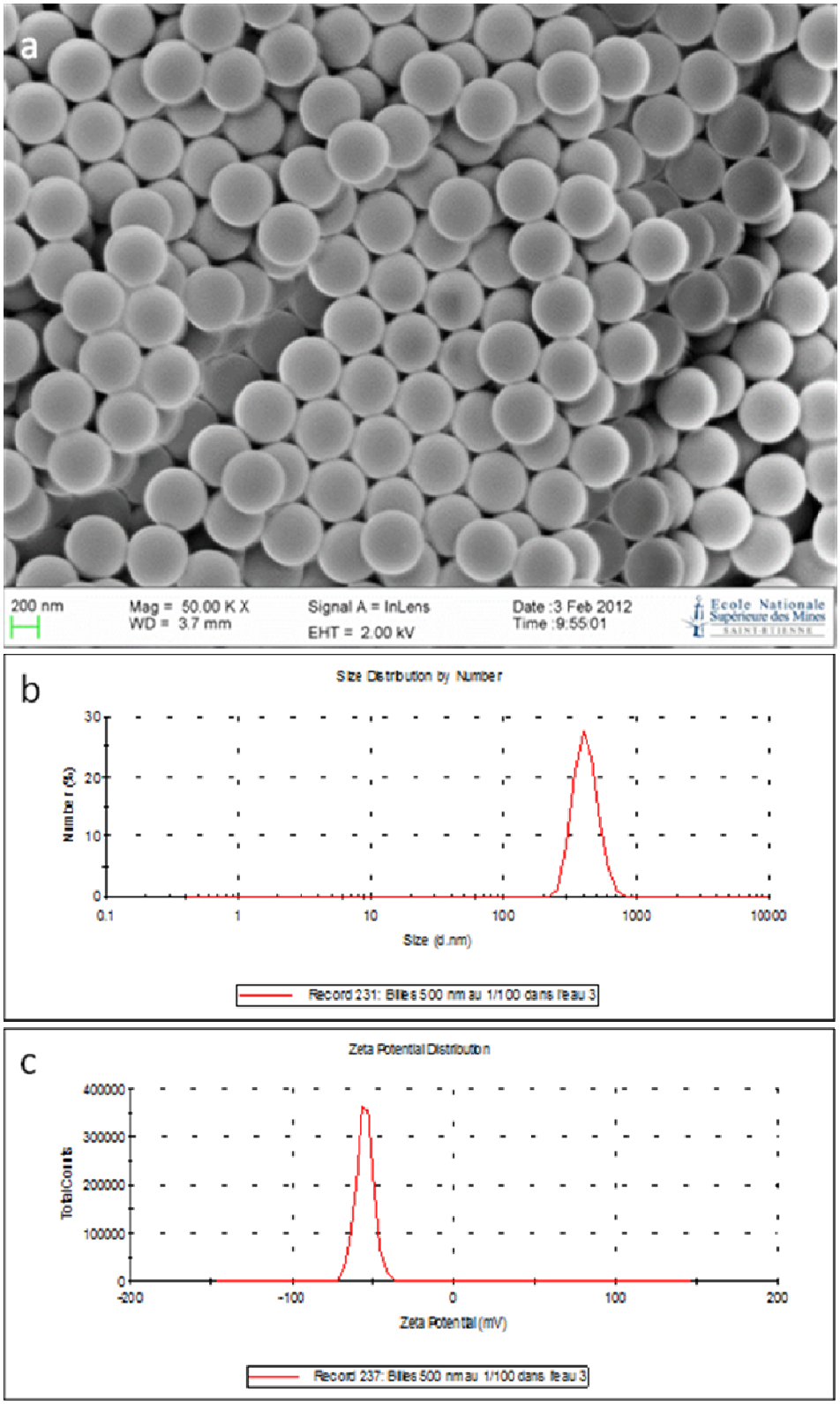

Fig. 1 Particle characterization. (**a**) Particles observed in scanning electron microscopy, ×50,000. (**b**) Size distribution and (**c**) zeta potential of particles in photon correlation spectroscopy

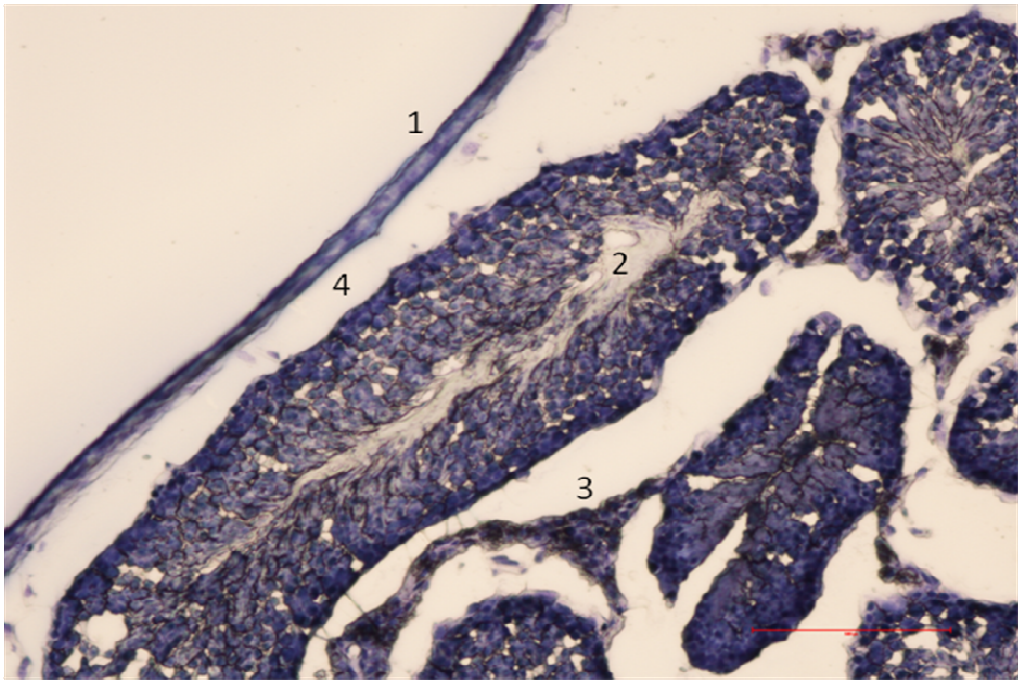

Fig. 2 Mouse testis stained with toluidine blue in optical microscopy, ×200. (1) Tunica albuginea; (2) seminiferous tubules; (3) interstitial spaces; (4) sub-albuginea spaces. Testicular structures were well preserved

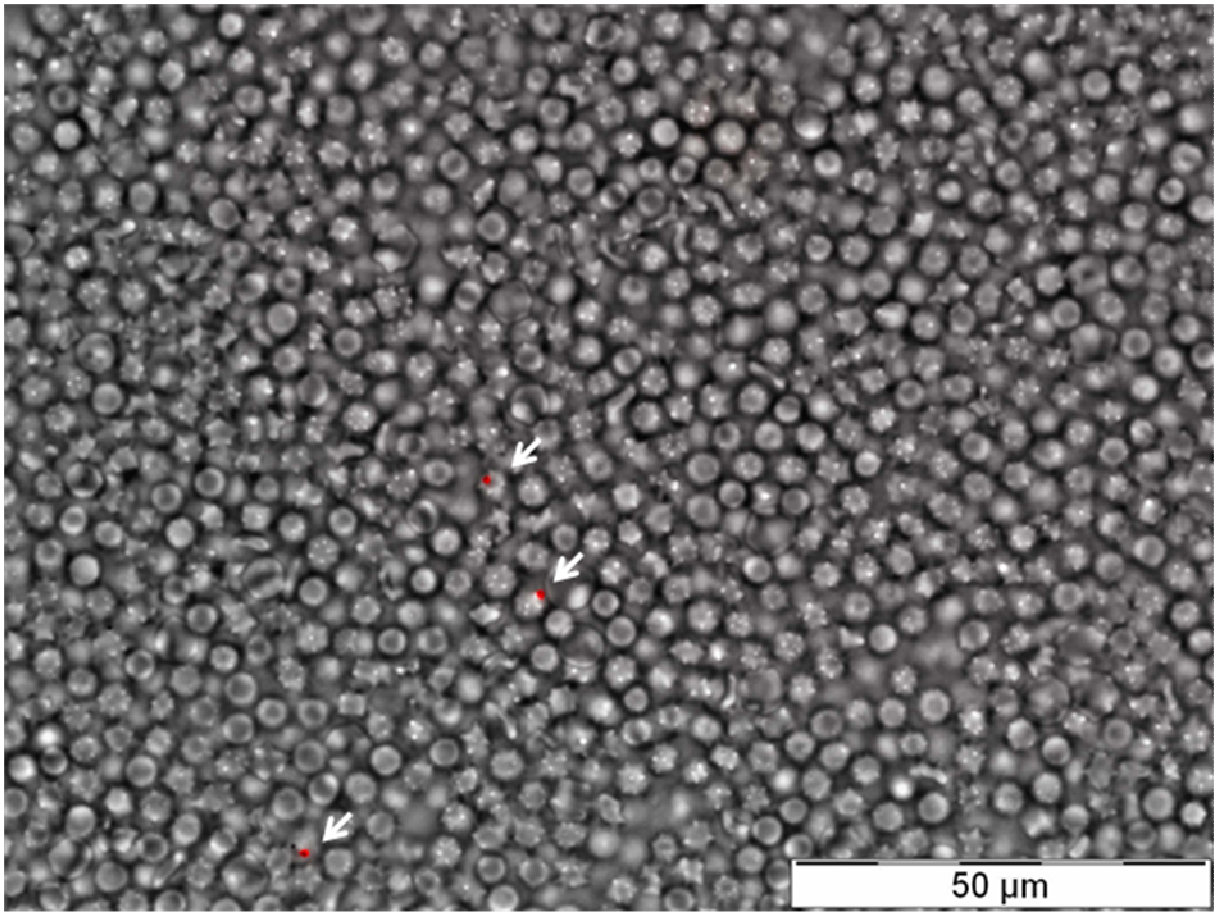

Fig. 3 Epifluorescence observation of D4 mice blood showing three fluorescent particles; red spectrum and brightfield, ×600

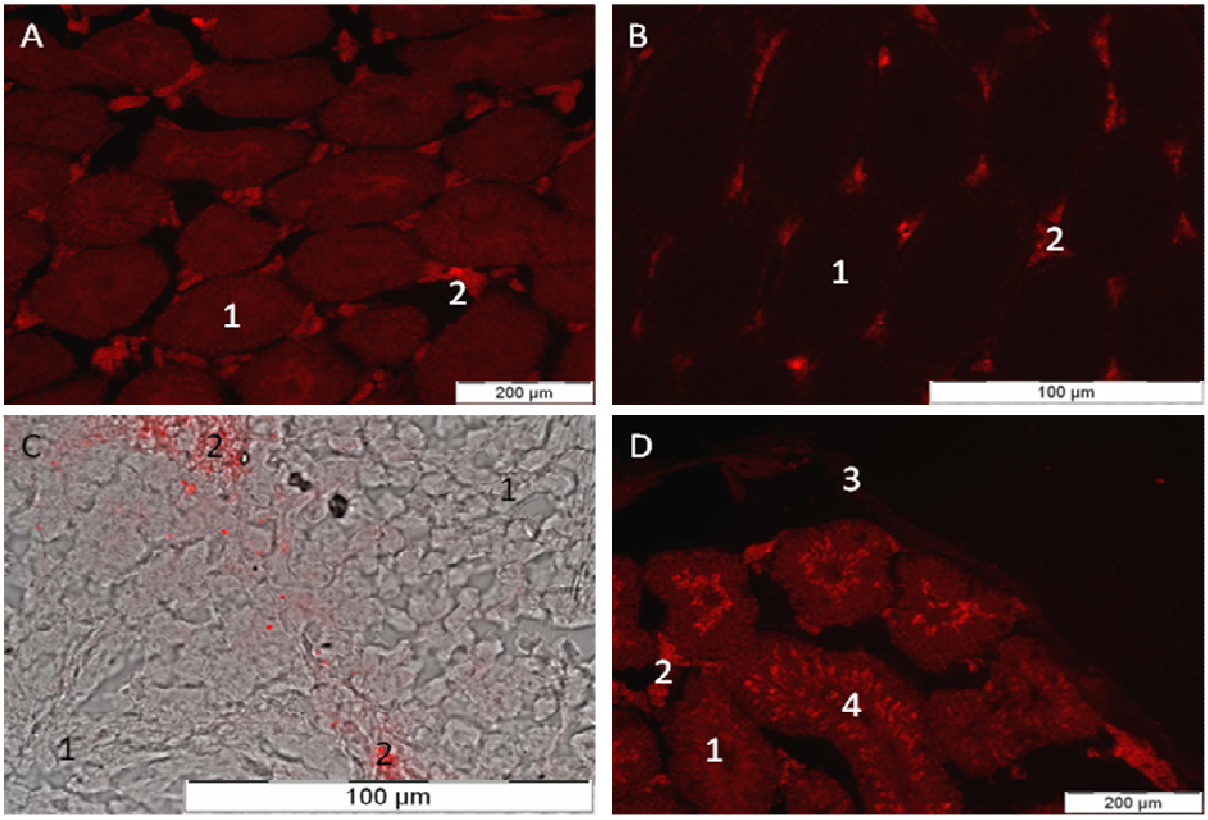

Fig. 4. Autofluorescence of control mice testes sections observed in epifluorescence microscopy. (**a, b and d**) red spectrum, ×100; (**c**) red spectrum and brightfield, ×600. (1) Seminiferous tubules; (2) interstitial spaces; (3) tunica albuginea; (4); spermatozoa in lumen of the tubules

Table 1 Number of particles found in the different parts of mice testes

	Control group (n = 40)	Time of sacrifice after injection				
		H1 (n = 30)	D4 (n = 30)	D21 (n = 30)	D45 (n = 30)	D90 (n = 30)
Tunica albuginea and sub-albuginea spaces	0	16	1	1	5	0
Interstitial spaces	0	4	3	2	5	1
Seminiferous tubules	0	1	0	3	4	0
Unknown	0	1	1	0	0	2
Total	0	22	5	6	14	3

n: number of sections obseved; (H1) 1 hour; (D4) 4 days; (D21) 21 days; (D45) 45 days; (D90) 90 days

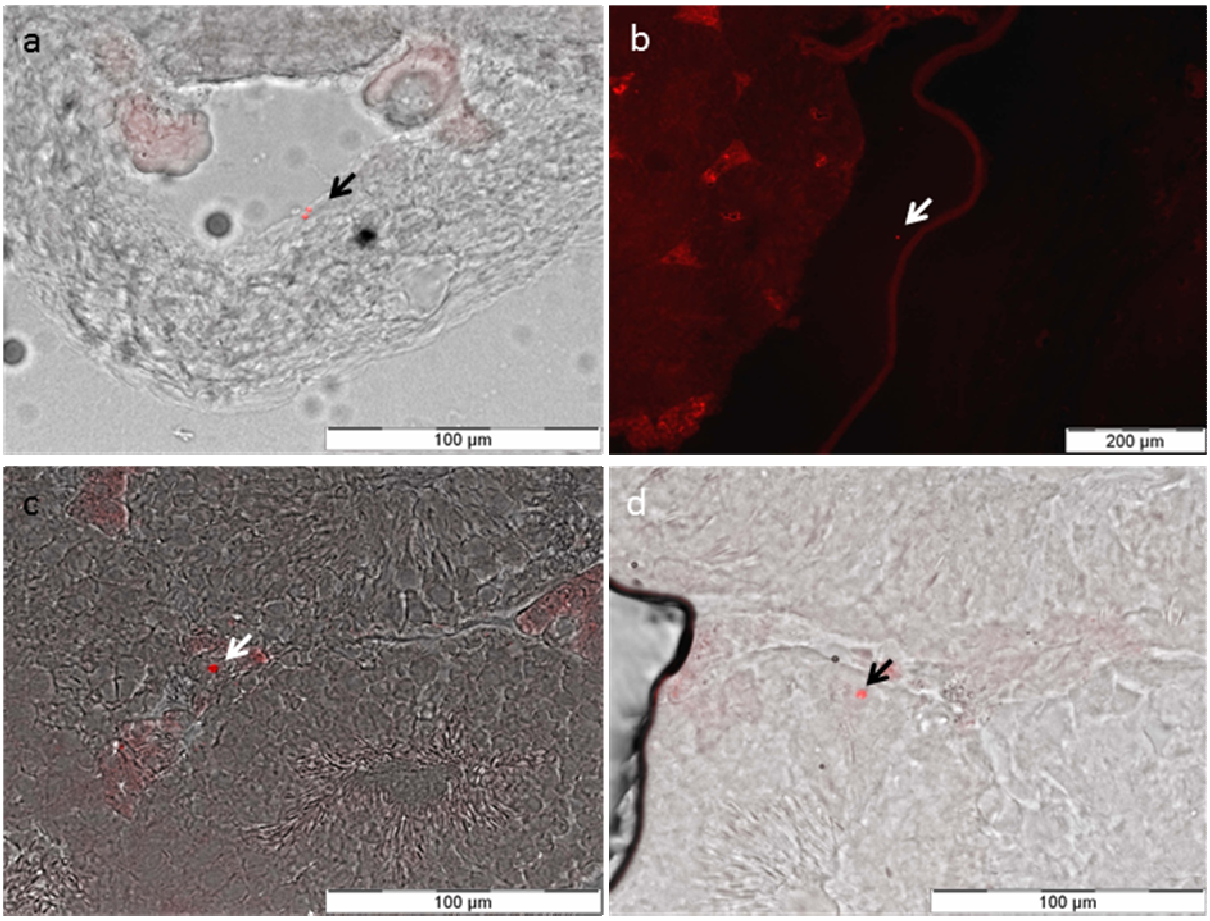

Fig. 5 Epifluorescence microscopy observation of mouse testis showing fluorescent particles. (**a, c and d**) red spectrum and brightfield, ×400; (**b**) red spectrum, ×100. (**a**) H1 group, 2 particles in the tunica albuginea; (**b**) D21 group, 1 particle in sub-albuginea space; (**c**) D4 group, 1 particle in interstitial space; (**d**) D21 group, 1 particle in a seminiferous tubule

Table 2 Number of particles found in mouse testes according to their distance from macrophages

Distance from macrophages	Control group (n = 10)	Time of sacrifice after injection					
		H1 (n = 15)	D4 (n = 15)	D21 (n = 15)	D45 (n = 15)	D90 (n = 15)	Total (n = 85)
Far	0	8	0	1	5	1	15
In contact	0	2	3	0	0	2	7
Inside	0	0	0	0	0	0	0

n = number of sections observed; (H1) 1 hour; (D4) 4 days; (D21) 21 days; (D45) 45 days; (D90) 90 days

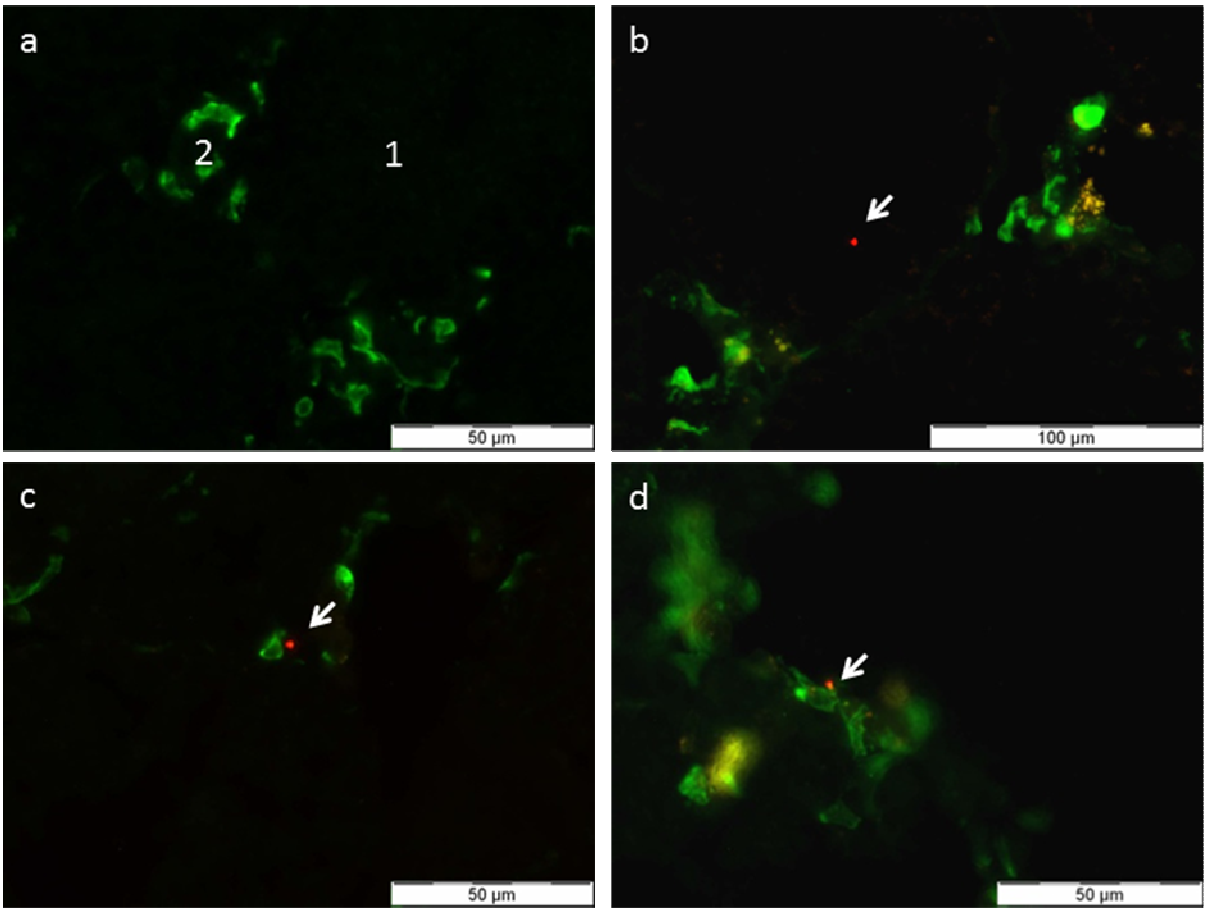

Fig. 6 Testicular sections after macrophage immunostaining with a green fluorescent dye. Spectrum red and green, ×400. (**a**) Control group, macrophages only lie in interstitial spaces and sub-albuginea spaces, not in seminiferous tubules; (**b**) D45 group, a particle in a seminiferous tubule far from macrophages; (**c**) H1 group, a particle in interstitial space but still at a distance from macrophages; (**d**) D90 group, a particle in contact with a macrophage. (1) Seminiferous tubules, (2) interstitial spaces

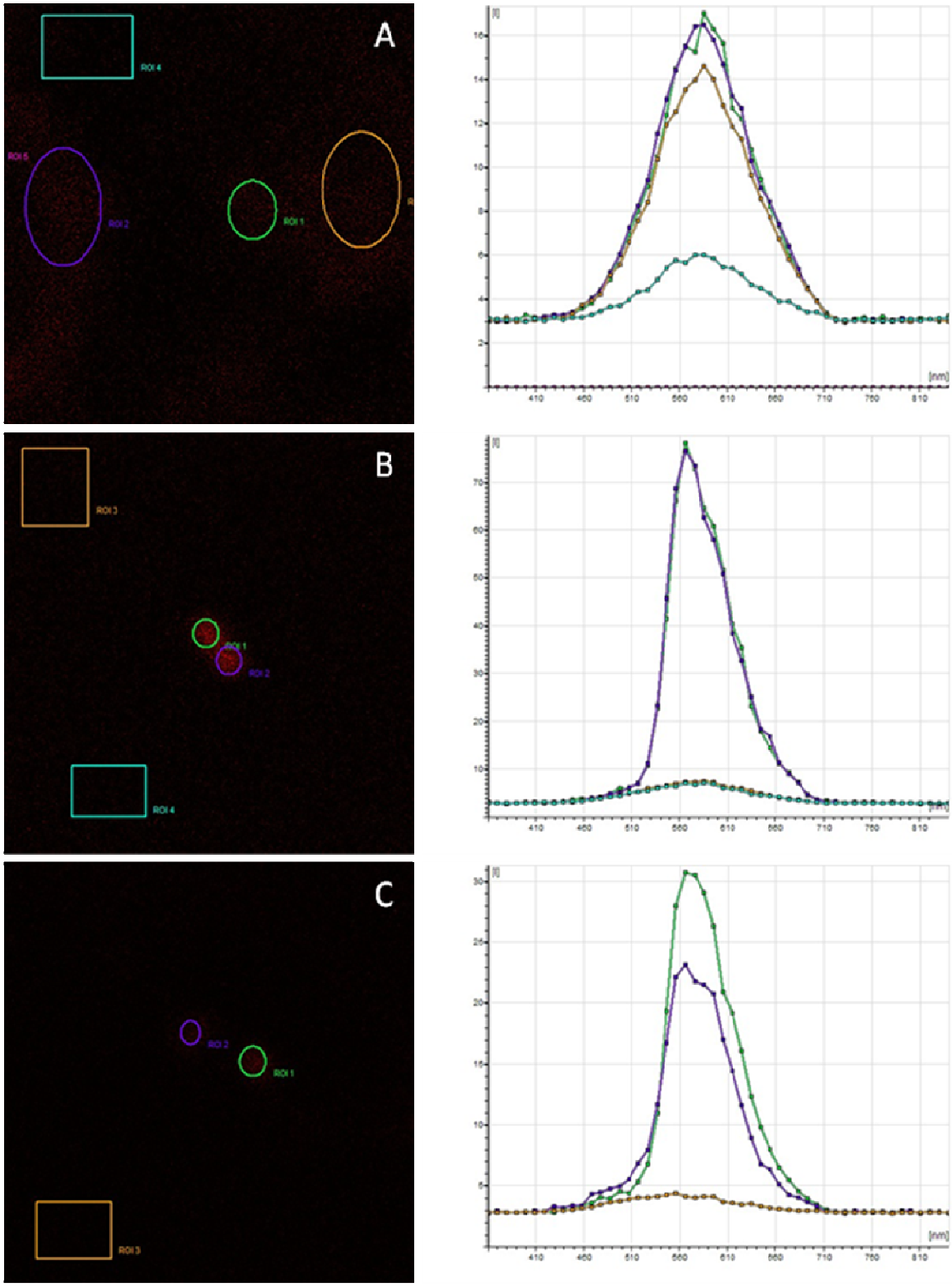

Fig. 7 Analysis of emission spectra in confocal microscopy. Left: observed section and analyzed areas. Right: emission spectra from 350 nm to 840 nm. (**a**) Control group; (**b**) control particles; (**c**) observed particles